REPORT DOCUMENTATION PAGE

Form Approved
OMB No. 0704-0188

Public reporting burden for this collection of information is estimated to average 1 hour per response, including the time for reviewing instructions, searching data sources, gathering and maintaining the data needed, and completing and reviewing the collection of information. Send comments regarding this burden estimate or any other aspect of this collection of information, including suggestions for reducing this burden to Washington Headquarters Service, Directorate for Information Operations and Reports, 1215 Jefferson Davis Highway, Suite 1204, Arlington, VA 22202-4302, and to the Office of Management and Budget, Paperwork Reduction Project (0704-0188) Washington, DC 20503.
PLEASE DO NOT RETURN YOUR FORM TO THE ABOVE ADDRESS.

1. REPORT DATE *(DD-MM-YYYY)* 12/08/99	2. REPORT DATE	3. DATES COVERED *(From - To)* 05/01/96 – 12/31/98

4. TITLE AND SUBTITLE

Accelerated Program Development of High-Quality, Large-Area GaN and AlGaN Substrates

5a. CONTRACT NUMBER

5b. GRANT NUMBER
N00014-96-1-0713

5c. PROGRAM ELEMENT NUMBER

6. AUTHOR(S)

J. F. Schetzina

5d. PROJECT NUMBER
98PR03283-00

5e. TASK NUMBER

5f. WORK UNIT

7. PERFORMING ORGANIZATION NAME(S) AND ADDRESS(ES)

North Carolina State University
Office of Sponsored Programs
Box 7514
Raleigh, NC 27695-7514

19991213 071

9. SPONSORING/MONITORING AGENCY NAME(S) AND ADDRESS(ES)

Office of Naval Research
Ballston Centre Tower One
800 North Quincy Street
Arlington, VA 22217-5660

10. SPONSOR/MONITOR'S ACRONYM(S)
ONR

11. SPONSORING/MONITORING AGENCY REPORT NUMBER

12. DISTRIBUTION AVAILABILITY STATEMENT

Approved for public release; distribution unlimited

13. SUPPLEMENTARY NOTES

The views, opinions and/or findings contained in this report are those of the author and should not be construed as an official ONR position, policy or decision.

14. ABSTRACT

The purpose of this work was to explore growth of thick layers of GaN, AlN, and AlGaN for use as substrates in III-N device epitaxy using sublimation vapor phase epitaxy (SVPE). The SVPE system was a vertical, cold-wall, pancake-style reactor similar in design to a MOCVD reactor. Ammonia was used as a nitrogen source, while the group III precursors were gallium chloride, $GaCl_3$, and aluminum chloride, $AlCl_3$. All growths were performed on sapphire substrates with ~1μm GaN buffer layers prepared by MOCVD..

15. SUBJECT TERMS

16. SECURITY CLASSIFICATION OF:			17. LIMITATION OF ABSTRACT	18. NUMBER OF PAGES	19a. NAME OF RESPONSIBLE PERSON J.F. Schetzina
a. REPORT	b. ABSTRACT	c. THIS PAGE		28	19b. TELEPONE NUMBER *(Include area code)* (919) 515-3314

DTIC QUALITY INSPECTED 3

Standard Form 298 (Rev. 8-98)
Prescribed by ANSI-Std Z39-18

Final Technical Report

DARPA/ONR Grant N0014-96-1-0713
"Accelerated Program Development of High-Quality, Large-Area GaN and AlGaN Substrates"

and

ONR/DURIP Equipment Grant N00014-97-1-0331
"Equipment for Bulk Crystal Growth of Aluminum Nitride"

J.F. Schetzina
Principal Investigator
Professor of Physics
North Carolina State University
PH: 919-515-3314; FAX 919-515-7667
e-mail: jan_schetzina@ncsu.edu

Summary

The purpose of this work was to explore growth of thick layers of GaN, AlN, and AlGaN for use as substrates in III-N device epitaxy using sublimation vapor phase epitaxy (SVPE). The SVPE system was a vertical, cold-wall, pancake-style reactor similar in design to a MOCVD reactor. Ammonia was used as a nitrogen source, while the group III precursors were gallium chloride, $GaCl_3$, and aluminum chloride, $AlCl_3$. All growths were performed on sapphire substrates with ~1μm GaN buffer layers prepared by MOCVD..

Gallium nitride layers up to 300μm thick were grown. The samples exhibited room-temperature photoluminescence peaks near 3.416 eV having a FWHM of 55 meV. X-ray rocking curves taken from the (0002) reflections had FWHMs as low as 274 arcsec. The surfaces of the GaN layers were not completely smooth, having hexagonal or "volcano" growth morphologies accompanied by scattered brown crystal "spires". Use of hydrogen carrier gas in the system instead of nitrogen improved the morphology of the films and eliminated many of the crystallites. Recent experiments performed near atmospheric pressure in a hot-walled reactor show further improvement in surface quality.

Aluminum nitride layers were grown with thicknesses up to 26μm. Room temperature cathodoluminsecence spectra show emission below the bandgap at energies between 5.714 and 5.891 eV. X-ray rocking curves having a FWHM of 484 arcsec were taken from (0002) reflections. Surface morphologies were generally smooth.

A small number of AlGaN samples were grown using both chloride materials simultaneously. Aluminum mole fractions between 0 and 16% were observed as measured by cathodoluminsecence. Surface features were similar to those found in the GaN experiments.

1. Introduction

1.1 Background

The class of III-V semiconductor compounds has been studied since the beginning of the semiconductor industry. These materials are denoted III-V because one of the elements in the binary compound, the cation, comes from group III in the periodic table, and the other element, the anion, comes from group V in the periodic table. Of the III-V materials, GaAs, AlAs, and InP, as well as their alloys, have been studied most extensively. Devices made from these compounds are optically active from the greenish-yellow to the infrared regions of the spectrum.

Interest in a subclass of the III-V compounds, the III-N semiconductors, has grown rapidly in recent years. The nitride materials GaN and AlN have bandgaps in the ultraviolet, 3.4 eV and 6.2 eV, respectively. InN has a bandgap of 1.9 eV, which falls in the red region of the spectrum. Therefore, alloys of these three materials can be optically active at wavelengths ranging from the red to the ultraviolet (Figure 1.1). This wide range makes the III-N compounds an obvious choice for use in optoelectronic devices such as light emitting diodes (LEDs), semiconductor lasers, and photodetectors. Currently, Nichia Chemical Industries has commercially available bright blue and green LEDs based on GaN/InGaN structures [1]. Nichia has also demonstrated a semiconductor laser based on InGaN/AlGaN/GaN that has an estimated lifetime of 10,000 hours operating under continuous wave conditions at room temperature [2]. Other commercially available devices based on GaN and its alloys include blue LEDs made by Cree Research Inc.

The advantages of GaN and AlN over other III-V semiconductors in certain device applications include the physical and electrical stability of III-N materials at high temperatures. The melting points of both compounds are well above 2000°C, although they start to lose nitrogen from the lattice at temperatures above 600-700°C [3]. In most semiconductors the electrical properties of the material are a strong function of the temperature. Due to the wide bandgaps of GaN and AlN, higher temperatures are not as detrimental to the electrical properties as they would be for narrower gap materials like GaAs. In particular, the intrinsic carrier concentration in GaN is so small that p-n junctions are viable at temperatures up to 500°C. For these reasons of stability, GaN and the alloy AlGaN are promising materials for high output microwave power devices.

One of the main factors that inhibit the quality of devices made from III-N materials is the lack of a lattice-matched substrate. The lattice is the array of positions in a crystal that the atoms occupy and is defined by the spacing of the lattice sites, called the lattice constant, and by the spatial orientation of the sites with respect to one another. A substrate is the base material upon which semiconductor films are deposited, and it is these thin layers which form the basis for semiconductor devices. To deposit the highest quality film, the lattice constant of the substrate material should exactly match that of the deposited layer. This is the case when the film and the substrate are of the same material and is called homoepitaxy. When the layer and substrate are of dissimilar materials, called heteroepitaxy, there is always some amount of lattice mismatch present. This is measured as a percentage difference between the lattice constants of the two materials. When the lattice mismatch between two materials is small, thin layers may be grown in which the lattice spacing of the film conforms to that of the substrate. These films are said to be in tension if the lattice constant of the layer is smaller than that of the substrate, or said to be in compression if the reverse is true. Once a critical film thickness is reached, however, the strain in the layer becomes too great and a further one-to-one relationship between the film lattice and substrate lattice can no longer be maintained. A defect in the layer near the interface then forms which allows the atoms of the film material to relax back to their preferred atomic spacing. The relaxation results in either an extra atom in the layer compared to the substrate in the case of tensile strain, or in a missing atom referenced to the substrate in the case of compressive strain. These defects

can be detrimental to the physical and electrical properties of the deposited films. Thus the growth of semiconductor films with good physical and electrical characteristics requires good lattice matching between the layers and substrate material.

Homoepitaxy offers the best solution to the problem of lattice mismatch. In many of the III-V semiconductor material systems, such as GaAs and InP, high-quality substrates of large dimensions (>2") are commercially available. This is not true for the III-N compounds. There exist no large-area bulk GaN or AlN crystals suitable for commercial substrate applications. Most GaN and related growths occur on sapphire (Al_2O_3) or silicon carbide (SiC) substrates. The mismatch between these materials and the III-N compounds can be quite large. For SiC the mismatch with GaN is 3.5% and for sapphire it is 16%. Films grown on these substrates have a large number of dislocations, from 10^8 to 10^{10} cm^{-2}, and special growth techniques are sometimes needed to get the films to even nucleate on the substrate medium. Even though commercialization of nitride LEDs grown on SiC and Al_2O_3 has been achieved despite the substrate issue, there are many other device applications where bulk nitride substrates are sorely needed. For example, photodetectors require high carrier mobilities and carrier lifetimes in order to achieve optimal efficiency and bandwidth. Carrier traps and recombination centers are detrimental to the electronic transport properties and typically arise from defects in the grown material. Thus there exists the need for GaN, AlN, and even AlGaN substrates of suitable quality and size to be used in device applications.

1.2 Statement of Purpose

The purpose of this work was to investigate the growth of GaN, AlN, and AlGaN substrates by modified Sublimation Vapor Phase Epitaxy (SVPE). This process used the high vapor-pressure solids gallium chloride ($GaCl_3$) and aluminum chloride ($AlCl_3$) as the group III precursors and ammonia (NH_3) as the nitrogen source. The majority of the growth experiments were conducted on 2" diameter sapphire wafers. The objective was to deposit thick layers of the nitride materials that could be used as substrates for device growth by molecular beam epitaxy (MBE) or metal-organic vapor phase epitaxy (MOVPE). The substrates could also be employed as seed crystals for homoepitaxial growth of more nitride substrates.

GaN, AlN, and AlGaN layers on the order of 5-300 µm thick were grown under various conditions and their physical and optical characteristics were studied in order to optimize the growth parameters. An optical microscope was used to examine the surface morphology of the layers. Sample surface features were also characterized by scanning electron microscopy (SEM). The crystalline quality was determined by double crystal x-ray diffraction (DCXRD). Optical characterization was done using photoluminescence (PL) and cathodoluminescence (CL).

Chapter 2 covers physical and optical properties of the group III nitrides, considers some of the current substrates for III-N epitaxy, and reviews the growth techniques for these materials. Chapter 3 describes the experimental setup and procedures. Chapter 4 discusses the thermodynamics of GaN and AlN growth employing chloride methods. Chapter 5 offers the results of this research. Chapter 6 draws conclusions from this work and provides possible directions for future investigation.

2. III-N Semiconductor Properties and Growth Techniques

2.1 Properties of III-N Materials

2.1.1 Crystal Structure and Thermal Properties

The materials GaN and AlN can exist in three different crystal structures: the wurtzite, zinc blende, and rocksalt configurations. The wurtzite structure is thermodynamically favored under ambient conditions, but GaN and AlN layers can be forced into the zinc blende structure when grown on (001) Si [4] or GaAs [5]. The rocksalt phase is only attainable under very high pressures [6,7].

The majority of work on III-N optoelectronic devices has been with wurtzite material. The conventional unit cell is based on the hexagonal close-packed (HCP) lattice (Figure 2.1). The wurtzite structure consists of two interpenetrating HCP cells offset by 3/8 of the height along the c-axis (Figure 2.2). The group III elements occupy one of the HCP lattices and the N atoms the other. Each atom is tetrahedrally bonded to four atoms of the opposite type and there are 6 atoms of each type contained in the conventional unit cell.

For wurtzite GaN, the room temperature lattice parameters are a_0=3.1892 ± 0.0009Å and c_0=5.1850 ± 0.0005Å [9,10]. The thermal expansion of a_0 in the range 300K to 900K is linear with a slope of +5.59x10^{-6}K^{-1}. The expansion of c_0, however, is super-linear with temperature with mean values of +3.17x10^{-6}K^{-1} for T=300-700K and +7.75x10^{-6}K^{-1} for T=700-900K [4]. For wurtzite AlN, the lattice parameters at room temperature fall in the range a_0=3.110 - 3.113Å and c_0=4.978 - 4.982Å [11-14]. The thermal coefficients over the range 300-1100K have mean values of 4.2x10^{-6}K^{-1} for a_0 and 5.3x10^{-6}K^{-1} for c_0 [15]. The room temperature thermal conductivity of GaN and AlN are 1.3 W/(cm•K) [16] and 2.0 W/(cm•K) [17], respectively. Some properties of the III-N compounds and other materials are shown in Table 2.1.

GaN and AlN have very high melting points compared to other semiconductor compounds. However, the stability of these materials below their melting points is not as great as one might expect due to the high nitrogen partial pressures over GaN and AlN at elevated temperatures. The equilibrium N_2 pressure over GaN at the melting point, approximately 2800 K, is projected to be 13 kbar [18]. For nitrogen over AlN at the projected melting point of 3500 K the theoretical equilibrium pressure is 100 bar [19].

2.1.2 Optical Properties

In their wurtzite phase, GaN and AlN are direct gap materials. That is, the minimum energy transition from the valence band to the conduction band occurs between the zero momentum point in each band. The band gap of GaN at 300K is 3.39 eV [9] and is 3.50 eV at 1.6K [20], both of which correspond to the near UV region of the spectrum. The bandgap of AlN at 300K is 6.2 eV [21], and at 5K is 6.28 eV [22]. For the alloy $Al_xGa_{1-x}N$ at room temperature, the bandgap E_g varies with the mole fraction x of Al and a band-bowing parameter b=1.0 as [23]:

$$E_g \text{ (eV)} = 6.2x + 3.39(1\text{-}x) - bx(1\text{-}x)$$

The index of refraction is a material property that plays a role in optoelectronic devices. The index of the material determines how light behaves within the different layers of the device as well as how light couples to the outside environment. For single crystalline GaN films, the index of refraction is approximately equal to 2.45 in the visible region of the spectrum [24], and decreases in the infrared to 2.1 at wavelengths about 2.0□m [25]. For crystalline AlN, the reported index for the visible spectrum varies from around 2.08 [26] to 2.15 [27].

2.2   Substrate Issues

The key issue in the growth of the III-N compounds has always been finding an appropriate substrate for epitaxy since no bulk nitride material is available. Many materials have been used as substrates: c-plane, r-plane, and a-plane sapphire (Al_2O_3); 3C, 4H and 6H silicon carbide (SiC); (100) and (111) gallium arsenide (GaAs); (001) and (111) silicon (Si); lithium gallate ($LiGaO_2$); and spinel ($MgAl_2O_4$) to name a few. The substrates used most successfully to date in wurtzite phase growth of GaN and AlN are c-plane sapphire and (0001) 6H silicon carbide. Both of these materials are available commercially as 2" wafers and the (0001) surfaces have a hexagonal symmetry similar to GaN and AlN.

The crystal structure of sapphire is not the wurtzite configuration, although it does have a degree of hexagonal symmetry. The typical wurtzite structure consisting of two interpenetrating HCP lattices is not valid for sapphire because of the 2:3 ratio of aluminum to oxygen. The Al_2O_3 structure requires that one Al HCP position out of every three in the wurtzite configuration is void of an atom in order to maintain the proper Al to O stoichiometry. The primitive unit cell is rhombohedral but the conventional unit cell is usually expressed in hexagonal form (Figure 2.3). C-plane sapphire, also denoted basal plane or (0001) sapphire, has the hexagonal surface that most readily supports deposition of wurtzite GaN and AlN. It has been found that deposition proceeds such that the (0001) plane of GaN/AlN is rotated 30° with respect to the sapphire (0001) surface [29]. This means that the crystallographic directions in the materials are related by:

$$[1\text{-}100]_{nitride} \parallel [11\text{--}20]_{sapphire}$$
$$[11\text{--}20]_{nitride} \parallel [1\text{-}100]_{sapphire}$$

Taking into account the rotational alignment leads to a lattice mismatch of 16% for GaN and 13% for AlN on (0001) Al_2O_3. This mismatch is very large and is one of the main factors that limits the crystalline quality of nitrides grown on sapphire.

GaN does not grow easily on the sapphire surface without some sort of pre-treatment of the substrate because it does not "wet" the sapphire at temperatures necessary for growth of good crystalline quality material. The result is that experiments performed on bare sapphire tend to have little deposition or deposition in the form of small individual hexagonal crystallites. In order to grow high quality material, in-situ substrate preparation is critical and methods can differ from one growth technique to the next.

Silicon carbide is the other widely used substrate for III-N epitaxy. It is a binary material that can exist in either zinc blende or hexagonal form. The zinc blende is typically denoted as β-SiC or 3C-SiC, the C standing for cubic. The hexagonal material, prefixed by α, shares the wurtzite nature of the nitrides with the exception of the planar stacking sequence. In nitride (wurtzite) crystals, the group III sites from one HCP lattice to the next always stack directly over one another, and the same is true for the N sites. When viewed from above, this structure has a series of vertical "voids" which occur in three out of the six sectors which make up the hexagonal lattice net (Figure 2.4). These empty positions comprise another set of potential HCP lattice sites that are equivalent to the two sets of occupied lattice sites. Hence there are three possible HCP nets that the atoms can physically occupy, the third being a 30° rotation of the second. The stacking sequence of the HCP sub-lattices determines the different forms, called polytypes, of silicon carbide. α-SiC that follows the stacking sequence (abac) is denoted 4H-SiC because the sequence repeats after 4 pairs of Si-C planes. 6H-SiC repeats its sequence of (abcacb) after 6 pairs of planes (Figure 2.5). The H in all cases denotes hexagonal material. Other stacking sequences are possible, but are less commonly used for nitride epitaxy. Both GaN and AlN will deposit directly onto 6H-SiC at typical nitride growth temperatures. GaN deposition in this fashion tends towards 3-D growth unless some

intermediate layer, typically AlN or AlGaN, is used [30]. Because 6H-SiC has a smaller lattice mismatch with GaN (3.5%) and AlN (1.0%) compared to sapphire, it would seem to be better suited for III-N epitaxy. However, it has only been recently that high quality 6H-SiC become available in 2" diameter wafers, and these wafers are very expensive.

When performing heteroepitaxial growth, thermal expansion differences between the film and substrate must be considered. Semiconductor film growth is performed at elevated temperatures, so during cool-down the two lattices are contracting at different rates due to the disparities in their thermal expansions. If the film is thin and the expansion coefficients are nearly the same, the film lattice will be distorted by a small amount. If the strain created by cooling is larger than some critical value, then the film (or potentially the substrate in the case of a thick layer) will fracture in order to relieve the large forces involved. Obviously, cracking is not a desirable trait in films for semiconductor devices. As can be see from Table 2.1, both sapphire and silicon carbide have significant thermal expansion differences with respect to GaN. Silicon carbide and AlN have a small difference in their coefficients, but sapphire differs greatly from AlN.

Another substrate property that can be an important consideration for fabrication of device structures is thermal conductivity. For example, high output power devices and laser diodes require heat sinking in order to improve electrical stability and increase device lifetime. The ability of the substrate to effectively conduct heat away from the active regions simplifies device packaging by allowing the substrate (backside) to be directly bonded to an appropriate heat sink. The alternative would be to bond the topside (film) of the wafer to the heat sink, thereby placing the active regions as close as possible to the heat sink but complicating the task of making the necessary electrical contacts to the top of the wafer. Thus using a substrate with a good thermal conductivity simplifies the processing and packaging of the fabricated devices. The thermal conductivity of SiC is almost ten times greater than that of Al_2O_3, meaning that silicon carbide would be a better choice for a substrate material where heat dissipation is critical.

The ability of the substrate to conduct electricity can also be important for device fabrication. When structures are grown on non-conducting material like sapphire, all electrical contacts for the device must be made to the topside. These contacts are typically made to different layers within the device structure, so that extra processing steps are required to uncover the desired layers. With a conducting substrate like n-SiC, one electrical contact can be made to the backside of the wafer, saving a processing step. However, the heterojunction band offsets between the III-N layer and the SiC should be considered because of the effect they can have on the electrical properties of the device.

From the previous discussion it is clear that concessions must be made when using either sapphire or silicon carbide as a substrate for growth of III-N devices. The best alternative would be the development of bulk GaN, AlN and AlGaN wafers of large diameter for use as substrates.
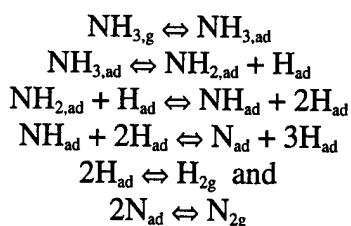
2.3 Growth Techniques

2.3.1 Overview

There have been many processes developed over the years to grow gallium nitride and aluminum nitride. One important consideration for III-N growth has always been the source of nitrogen atoms needed to react with the group III metals. The difficulty is that nitrogen occurs as a diatomic molecule (N_2) instead of individual atoms, and the binding energy of the molecule is very large, about 9.5 eV. This strong binding renders the N_2 molecule highly inert under most conditions. In order to generate a more active nitrogen species, plasma sources are often used in low-pressure growth processes. The plasmas are either generated by radio-frequency excitation (rf) or by electron-cyclotron resonance (ECR). Both methods convert a fraction of the N_2 molecules into high-energy nitrogen atoms or ions that can be utilized for film growth.

Several growth techniques use ammonia (NH$_3$) as a nitrogen source. With a binding energy of 4.8 eV, the ammonia molecule is more reactive and easier to thermally decompose than the nitrogen molecule. Ammonia thermally decomposes into N$_2$ and H$_2$ according the reaction:

$$NH_3 \Rightarrow 1/2N_2 + 3/2H_2$$

When thermal cracking of NH$_3$ occurs on the growth surface, the dissociation can be described by [31]:

$$NH_{3,g} \Leftrightarrow NH_{3,ad}$$
$$NH_{3,ad} \Leftrightarrow NH_{2,ad} + H_{ad}$$
$$NH_{2,ad} + H_{ad} \Leftrightarrow NH_{ad} + 2H_{ad}$$
$$NH_{ad} + 2H_{ad} \Leftrightarrow N_{ad} + 3H_{ad}$$
$$2H_{ad} \Leftrightarrow H_{2g} \text{ and}$$
$$2N_{ad} \Leftrightarrow N_{2g}$$

(g $\equiv$ gaseous, ad $\equiv$ adsorbed)

Note that in the fourth step atomic nitrogen is adsorbed on the surface. If the residence time is long enough for some of the N atoms to bond to Ga atoms on the surface before combining with another N atom (final step), then GaN can be formed using NH$_3$ as a source of nitrogen atoms.

The standard bulk-crystal growth techniques employed for many semiconductors, including Si and GaAs, are growths from the stoichiometric melt. In the Bridgman method the molten material is held in a long crucible and is slowly cooled from one end. This causes crystallization to begin in the cooler region and can be enhanced by the use of a seed crystal. The Czochralski method employs such a seed at the end of a vertical rod that is immersed in the melt. As the rod is withdrawn the surface tension of the liquid causes some of the material to adhere to the seed which then crystallizes as the rod is slowly removed from the melt. Unfortunately the high N$_2$ overpressures that are required at the melting points of GaN and AlN render these standard techniques impractical if not impossible.

2.3.2 Molecular Beam Epitaxy

Molecular Beam Epitaxy (MBE) is one of the most common methods for growing III-N compounds in research laboratories. MBE systems are ultra-high vacuum chambers in which several beams of atoms or molecules converge on a heated substrate to form the desired semiconductor compound. The molecular beams can be gaseous in nature, like N$_2$ or NH$_3$, or can arise from the sublimation (or vaporization in the case of liquids) of ultra-pure elemental or compound material contained in Knudsen-style furnace cells. MBE growth is a non-equilibrium process and, as such, employs lower substrate temperatures than other methods whose processes are closer to equilibrium. The growth chamber is maintained at a very low pressure, typically 10^{-10} torr. MBE growth rates tend to be rather low, on the order of 0.3 to 1.0 $\square$m/hr for III-N materials. This low deposition rate makes MBE an excellent choice for applications where precise control of interfaces and layer thickness are critical, but inappropriate for the growth of thick material.

2.3.3 Metal-Organic Vapor Phase Epitaxy

The most commercially successful growth method used for III-N material is Metal-Organic Vapor Phase Epitaxy (MOVPE). In contrast to MBE, MOVPE reactors operate in a much higher-pressure regime, from 10 to 760 torr, and with higher substrate temperatures. The source gases as well as inert "carrier" gases enter the chamber in a carefully controlled injection process and flow in a uniform manner to the heated substrate. Chemical reactions occur at the surface that result in film deposition. The metallic species are delivered to the substrate not as atoms but as molecules in which

the metal atom is bonded to an organic radical. These precursor molecules belong to a class of compounds named organo-metallics, and are also commonly called metal-organics. The precursors exist as either solids or liquids and have moderate to high vapor pressures near room temperature. The metal-organic containers are kept in constant-temperature baths and their vapors are transported to the reaction chamber by an inert carrier gas.

One feature that MOVPE shares with MBE is a slow growth rate. While the deposition rate for MOVPE is somewhat higher, from 0.5 to 4.0 $\Box$m/hr, it is still rather low to be considered for bulk or "quasi-bulk" growth where wafer throughput is an issue. Another more serious factor is the cost of the organo-metallics used as precursors. Typically 100g of trimethylgallium, which could grow 5.9mm of material on a 2" wafer assuming 100% efficiency, can cost several thousand dollars. Thus the high cost associated with each growth rules out MOVPE as a method for producing bulk material.

2.3.4   Ga + NH$_3$ Method

The earliest published reports of GaN growth utilized the direct reaction between heated gallium and ammonia gas [32,33]. With this technique, small platelets and needles of GaN were fabricated. AlN powder was also formed in a similar process by early researchers [34]. The growth reaction is simply

$$X + NH_3 \Rightarrow XN + 3/2H_2$$
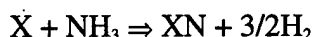
where X represents Ga or Al. The reaction requires temperatures high enough for some of the ammonia to dissociate. Logan and Thurmond [35] used 1cm^2 sapphire substrates placed into a Ga or Ga/Bi melt under an NH$_3$ environment to grow GaN at 1050°C. More recently, Fischer et. al. [36] have developed a technique where a heated 2" wafer is held suspended above a boat of molten gallium with a small temperature gradient between the two regions. Ammonia is passed through the space separating the substrate and the molten metal. The thermal gradient provides mass transport of gallium to the substrate, and decomposed ammonia provides atomic nitrogen to form GaN. The growth is performed at temperatures near 1240°C with a maximum growth rate of 250μm/hr.

2.3.5   Ga + N$_2$ at High Pressures Method

As mentioned previously, GaN and AlN are not expected to grow effectively from their stoichiometric melts. However, at least one group [37,38] has been able to demonstrate small shards and platelets a few millimeters in size crystallized from liquid gallium under high N$_2$ pressures. They are also able to grow AlN powder by a similar process. For GaN crystals, the growth temperature ranges from 1300-1600°C at N$_2$ pressures between 8-20 kbar. Small crystals and those with growth rates below 0.1mm/hr are of high structural quality, whereas larger samples and those with higher growth rates are of lower quality. One limitation on the crystal size stems from the small size of the growth chamber. The growth rate is hindered by the low solubility of the nitrogen in molten gallium.

2.3.6   Hydride Vapor Phase Epitaxy

Hydride Vapor Phase Epitaxy (HVPE) was the first technique that was able to deposit GaN and AlN epitaxially over large-area wafers. Maruska and Tietjen [39] deposited the first single crystal thin films of GaN by HVPE, and Chu et. al. [40] accomplished the same for AlN using a related technique. HVPE utilizes a chloride transport method in which HCl gas is passed over hot gallium to form gaseous GaCl. This binary vapor is then carried to the reaction zone where it reacts with ammonia at the substrate to deposit GaN. The process is carried out near atmospheric pressure in a hot-walled chamber. AlN can also be grown in this manner using liquid Al instead of Ga as the group III reactant. Due to the corrosive nature of the HCl gas and the need for the reactor walls to withstand the growth temperatures,

HVPE is performed in a quartz chamber. The tubular reactor is usually heated in a multi-zone furnace so that the substrate and the gallium source material can be kept at optimum temperatures (Figure 2.6).

A variation on the HVPE technique employs gallium trichloride ($GaCl_3$) and aluminum trichloride ($AlCl_3$) instead of liquid group III materials and HCl [3,21,41-43]. The precursors are carried from a heated container to the quartz chamber by an inert carrier gas. Groups have also grown AlN using a complex of ammonia and aluminum trichloride of the form $AlCl_3 \bullet nNH_3$ [43,44].

Growth rates for HVPE fall within a range of about 10-200 µm/hr. Like the method utilizing direct reaction with ammonia and gallium, HVPE requires a substrate on which to deposit the epitaxial layers. Due to lattice mismatch and thermal expansion differences between the epitaxy and the substrate, cracking of thick films is a problem in both of these growth systems.

3. Experimental Equipment and Procedure
3.1 Sublimation Vapor Phase Epitaxy
3.1.1 Growth Chamber

The Sublimation Vapor Phase Epitaxy (SVPE) system, designed and built at North Carolina State University, is an attempt to utilize a low-pressure MOVPE reactor to deposit thick GaN and AlN using a growth method related to HVPE. The main chamber is a vertical, cold-wall, pancake-style reactor capable of deposition on single wafers up to 3" in diameter (Figure 3.1 – 3.3). It is mated, via a UHV transfer line, to a cluster tool (Figure 3.4) that at present includes a MOVPE reactor (Figure 3.5), a MBE system (Figure 3.6), an Auger Electron Spectroscopy chamber, and a hydrogen-plasma cleaning station, all of which are dedicated to III-N compounds. Also connected to the SVPE system is a small chamber containing a turbomolecular pump and a Residual Gas Analyzer (RGA), the former used for pump-down of the chamber to a level compatible with the cluster tool, and the latter for gas sampling and chamber leak checking.

The sample mount used in the system is designed for both high rotation and high temperature. Since high rotation is typically used in low pressure MOVPE, the stepper motor/feedthrough assembly is designed to be operated at rotations up to 1500 rpm. Because AlN is usually grown at high temperatures, the sample mount is designed to heat the substrate to temperatures above 1200°C.

The process pump used during growth is a dual-stage rotary vane pump manufactured by Alcatel Vacuum (model 2063CP+) with a pumping speed of 50cfm. A MKS Model 653B throttle valve is placed at the inlet of the pump to provide control of the chamber pressure during growth. Also in the pumping lines between the chamber and the throttle valve are two items to remove vapors and particulates from the gas stream before entering the pump. The first and closest to the chamber is a two-stage cold trap. The first half contains water-cooled coils made out of stainless steel tubing wound in a toroidal shape and whose function is to condense out chloride compounds onto the coils. The second stage is a series of 28 screen wires whose purpose is to create turbulence in the lower part of the trap and promote further condensation of chloride species out of the outlet gas stream. The second item is an Alcatel particle filter that is used to remove dust from the gas stream. This filter is the last line of defense and is placed just before the throttle valve.

3.1.2 Source Gases and Flow Control

The gases used in the growth process are nitrogen, hydrogen, and ammonia. The nitrogen gas is Ultra-Pure Carrier (UPC) grade, corresponding to 99.9995% purity, supplied by Air Products. Prior to reaching the system flowmeters the nitrogen is passed through a Millipore resin-based in-line purifier for inert gases (part # WPMV200SI) to remove oxygen, water, and CO_2 to levels below 1 ppb. A palladium diffusion cell is used to purify hydrogen of moderate (99.995%) purity for use in the growth experiments. The palladium alloy cell, manufactured by Johnson Matthey (model HP-50), can purify high flows of H_2 gas to levels below 1ppb. "Blue" Ammonia from Solkatronic Chemicals is used due to its ultra-high purity, better than 99.9999%. It is passed through a Millipore purifier for hydride gases (part #WPMV200SH) to obtain impurity levels less that 1ppb.

Gas flows into the growth chamber are regulated by flowmeters manufactured by MKS Industries. Each flowmeter is isolated from the growth chamber by at least one pneumatic valve. At the chamber injection point for ammonia (and its carriers) there are two valves, one which allows flow into the chamber and the other which allows flow into a bypass line that leads directly to the process pump. Thus gas flows can be initiated and stabilized to their run values before being switched into the chamber.

The top flange of the system houses four VCR fittings that serve as gas input points. One fitting is for the gallium precursor input, one is for the aluminum precursor input, and two are for the ammonia

and its carrier. A fifth input, added later, serves as a chamber purge. All input lines were heated to 225°C from the chamber fitting up to the input valve to prevent condensation of the group III precursors.

3.1.3 Group III Precursors

The materials used as precursors for gallium and aluminum are gallium(III) chloride ($GaCl_3$) and aluminum(III) chloride ($AlCl_3$). These compounds are solids at room temperature and have significant vapor pressures at temperatures below 150°C. Both of these materials react strongly with water vapor to form HCl gas, so handling of these compounds is best done in a dry, inert gas environment.

Gallium(III) chloride is a white solid that melts near 80°C. The material used in this study was purchased from Alfa/ÆSAR in glass ampoules containing 100g of 99.999% purity material. The vapor pressure as a function of temperature for $GaCl_3$ is shown in Figure 3.7 [45] and can be approximated for a temperature T between 48°C and 132°C by:

$$\log P \text{ (torr)} = -7.5838 + 4.5274 \log T$$

The vapors of gallium chloride at low temperature are of the form $(GaCl_3)_2$, which dissociates into $GaCl_3$ molecules at temperatures above 400°C [46].

Aluminum(III) chloride is a powdery white solid similar in reactivity to gallium(III) chloride. Material of 99.99% purity in sealed glass jars was purchased from Alfa/ÆSAR. The vapor pressure of $AlCl_3$ (Figure 3.8) is lower than that of $GaCl_3$ until temperatures above 170°C are reached, at which point aluminum chloride has the higher pressure. The pressure as a function of temperature is given approximately by:

$$\log P \text{ (torr)} = -21.303 + 10.668 \log T$$

The melting point of aluminum chloride, 192.6°C, is only attainable at raised pressures. Like gallium chloride, the vapors of $AlCl_3$ are dimers at low temperatures that break up into individual molecules near 800°C [47].

To house the chloride compounds and deliver them to the growth chamber, special source containers were fabricated. Each source is a cylindrical stainless steel container topped with a 4.625" Conflat flange that has three VCR connections. These VCR ports are mated to pneumatic valves that sit on top of the source. One valve is used as an inlet for the carrier gas; one is used as the outlet to the chamber; the third opens to a bypass line that ends at the cold trap. Thus the carrier flow into and out of the source can be stabilized employing the bypass line before being switched into the chamber. Between each valve and the top flange is a 0.25" thick block of aluminum in which a 100W cartridge heater is housed. Together with a thermocouple in one of the aluminum pieces, the three heaters are used to control the temperature of the source. All of the heat is supplied to the valves and the top of the source in order to minimize condensation of the chloride materials and avoid blockage of the source lines and valves. The canister and valves are insulated to minimize heat loss. The chloride powder sits at the bottom of the source in a Pyrex liner capable of holding 400g of material.

Calculating the flux of chloride vapors out of the sublimation sources from the material temperature and carrier gas flow is not straightforward. Under equilibrium conditions the canisters can be modeled after MOVPE "bubblers" so that the outgoing flux ϕ_s of chloride material in mmol/min is given by:

$$\phi_s = F_c P_s / ((P_T - P_s)/22.4)$$

F_C = carrier gas flow in sccm
P_S = partial pressure of source material
P_T = total pressure in the source container

However, this formula is not valid for the solid sources because they are normally operated in the regime where P_S is between 10% and 40% of P_T. Therefore, the steady state vapor pressure of the chloride is much less than P_S because the vapors can not maintain equilibrium with the solid/liquid. In order for the flux equation to be valid, the steady state pressure P_{SS} (which is likely a function of the carrier gas flow) must be used in place of P_S. It is necessary in the calculation to estimate the value for P_T because there is no direct measurement of the total source pressure. Direct control of the pressure is difficult because of the necessity of heating all lines coming from the source and the corrosive nature of the source material. The pressure in each source is essentially the chamber pressure plus a small amount to account for the carrier gas flow through the source. Another complication in the flux calculation is that the source temperature is measured at the top of the canister, which means the chloride inside must be at a lower temperature. It is thus necessary to estimate the temperature drop in order to determine P_{SS}.

Due to the corrosive nature of chlorine-containing compounds, there are a limited number of construction materials that can be used when employing chlorides. Fortunately the nickel-containing stainless steels (304, 316L) used standard in UHV chambers are suitable for this purpose. However, under a constant environment of hot chloride vapor, stainless steel is susceptible to stress corrosion cracking. This occurs when chlorine attacks the stainless steel at grain boundaries and causes cracking and fracturing in the material. Especially susceptible are the weld joints in the steel since the residual strain contained in the weld can help promote the formation of cracks. Teflon coating on the walls and tops of the sources is used as protection from constant exposure to heated $GaCl_3$ and $AlCl_3$ vapors. The valves used on the sources are made out of Monel to better withstand the heating of the source and the corrosive nature of the chlorides.

3.2 SVPE Film Growth

The majority of samples described in this work were grown on 2" diameter sapphire wafers with 1μm of GaN pre-deposited by MOVPE. These GaN buffer layers were initially provided by Cree Research Inc. of Durham, N.C. More recently, the buffer layers were fabricated at N.C. State utilizing the MOVPE reactor that was added to the laboratory. All samples had 0.6μm of molybdenum sputtered onto the backside to improve the thermal contact between the wafers and the sample block. Unless otherwise noted, the term "substrate" will refer to 2" sapphire having GaN buffer layers, regardless of the wafer source.

Prior to growth, substrates were degreased sequentially in acetone and methanol in an ultrasonic bath and blown dry with filtered N_2. They were then mounted on a molybdenum sample block capable of holding 3" wafers. Samples were held in a 0.009" deep recess in the moly block by four 0.010" thick moly "legs". The legs, 0.062" by 0.375", were tied down to the block by 0.005" diameter tantalum wire. The substrates were then placed in the load-lock for the UHV transfer line and pumped below $1x10^{-8}$ torr before transfer into the SVPE reactor.

Once in the main chamber, the sample was spun up to the growth rotation speed, 20 to 1000 rpm, while under vacuum. Once full rotation speed was achieved, the growth chamber was switched from the turbomolecular pump to the process pump. Next, nitrogen purge flows (150–200 sccm) for the viewports, feedthroughs, and gate valves were initiated. The flows for ammonia (0.1–9.0 slm) and the carrier gas (nitrogen and/or hydrogen at 0–10.0 slm) were then established at their growth values. The main chamber pressure was set to the run value, from 1 to 600 torr. The sample was then ramped to the

growth temperature at a rate of 40 to120°C/min. The substrate temperature was measured with an Ircon optical pyrometer focused through a sapphire viewport.

When the substrate temperature reached the setpoint and the pyrometer reading had stabilized, the chloride carrier gas flow was sent through the source and into the bypass lines to the cold trap. Once the flow through the source had stabilized to the run value, the bypass valve was closed and the chamber valve was simultaneously opened to allow the growth to begin. Typical growth times were one hour.

At the end of the growth, the chloride carrier gas flow was switched from the chamber to the bypass lines and then turned off. The sample was ramped down from the run temperature to 500°C. During this first cooling phase the ammonia flow was gradually reduced as the sample temperature dropped until the flow was set to zero at a temperature near 650°C. From this point on only nitrogen was flowing into the chamber. When the sample had reached 500°C the chamber pressure was lowered to 1 torr and a second, slower temperature ramp was initiated that took the wafer from 500°C to less than 100°C in about two hours. The purpose of this slower ramp under nitrogen flow was to purge out the ammonia and chloride compounds that accumulate on the cold chamber walls that could act as major outgassing sources when pumped on with the turbomolecular pump. Once the chamber was sufficiently evacuated the sample could be transferred into the UHV transfer line and, from there, into the load-lock for removal.

3.3 Characterization of SVPE Films

In order to evaluate the quality of grown layers, optical and physical characteristics of the films were measured. The techniques employed were optical microscopy, scanning electron microscopy, photoluminescence, cathodoluminsecence, and double crystal x-ray diffraction.

The first phase in evaluating the quality of the films was to examine their morphology. Surface features of the samples were viewed with an Olympus BX60 optical microscope capable of brightfield, darkfield, and Nomarski imaging. Magnifications ranged from 45X to 1500X. Images of some samples were also taken in a JEOL JSM 6400 Scanning Electron Microscope with a JEOL DSG digital imaging system. Films should have a smooth surface free of pits and hillocks and be transparent to visible light. Thin films should be free of cracks, but those above about 10μm thickness are expected to have observable cracks due to the difference in thermal expansion between the grown layers and the sapphire substrate.

Photoluminescence (PL) occurs when a photon whose energy is greater than the bandgap is absorbed by the material, resulting in emission of a photon whose energy is near or less than the bandgap. The plot of the intensity versus wavelength for light emitted by the sample under irradiation by a monochromatic light source is called the photoluminescence spectrum. The samples in this study were measured at room temperature using the 325nm line of a Liconix Model 4300 HeCd laser with an output power of 15 mW. Emission from the layers was focused into an optical fiber and coupled to an Acton Research Corp. SpectraPro 500 triple grating spectrometer and a Princeton Instruments RY-1024 diode array. Ideally the spectrum should consist of a single, intense, narrow peak near the band edge. Other peaks at lower energies may be present and can signify defects or impurities within the film. The measurement of the peak width is given as the Full Width at Half Maximum (FWHM) in units of nm (wavelength) or meV (energy). Photoluminescence was performed only on GaN samples because the 325nm HeCd emission falls well below the bandgap of AlN. Also, PL was not practical for AlGaN films since the optics used to filter out the reflected HeCd laser emission interfered with the detection of emission at energies higher than ~3.4eV.

Cathodoluminescence (CL) is similar to PL with the difference that the excitation of the sample occurs by irradiation with a beam of high-energy electrons (5-25kV) in vacuum. The electrons impart energy to the sample lattice that results in emission of photons. Thus this process is an effective way to

record the emission spectrum of samples with large bandgaps, like AlN and AlGaN. The CL spectra were recorded in the JEOL Scanning Electron Microscope with an Oxford Research MonoCL diffraction grating and photomultiplier tube assembly.

The crystalline quality of the grown layers was evaluated with a Phillips PW1729 x-ray generator coupled with a Blake Industries double crystal diffractometer. The x-ray source tube employed a beam at a wavelength of $\lambda=1.540562A$ (the Cu K_α line). This double crystal technique utilizes a high-quality substrate as the first crystal in the x-ray path, where the second crystal is the sample being measured. Ideally the first crystal should be the same material as the sample being measured, but since no bulk GaN was available, a SiC substrate with a 1μm GaN epilayer was used. Exit slits from the first diffractometer were set to the universal standard 1mm x 1mm. Diffraction intensity from the (0002) crystal planes of the sample was measured as the sample was rocked about the (0002) peak angle. Narrow diffraction peaks indicate high crystalline quality material, whereas broader peaks are indicative of lower quality material. The measurement of the peak width is given as the FWHM in units of arcseconds.

4. Thermodynamics of VPE Using Trichlorides

4.1 Review of Thermodynamics

In the thermodynamics of semiconductor film growth the important quantity is the change in the Gibbs free energy of the system. The Gibbs energy G is defined as

$$G = H - TS$$

where H is the enthalpy, T the temperature, and S the entropy. This definition applies to a homogeneous system at uniform temperature. If the reaction in question is carried out at constant temperature then the change in free energy is given by:

$$\Delta G = \Delta H - T\Delta S$$

Note that both ΔH and ΔS are also functions of T. In order for the reaction to proceed spontaneously ΔG must be less than zero. The more negative ΔG, the stronger the thermodynamic driving force for the reaction to occur. However, the size of ΔG is irrelevant to the speed of the reaction. Thus a reaction can be thermodynamically favorable and, even with a large driving force, still proceed slowly. The rate at which the reaction occurs can only be determined empirically.

Consider the balanced chemical reaction:

$$aA + bB \Leftrightarrow cC + dD$$
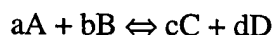
The capital letters indicate chemical species and the corresponding lower case letters are the coefficients necessary to balance the reaction. To simplest way to calculate ΔG for a given reaction is to use the free energy of formation, ΔG_f. Values of ΔG_f represent the change in Gibbs free energy that occurs when a compound is formed from its constituent elements in their standard states. For ammonia, $\Delta G_{f,NH3}$ is the change in free energy when 1 mol of NH_3 is formed from 0.5 mol of N_2 gas and 1.5 mol of H_2 gas. The Gibbs energy change for a general chemical reaction, ΔG_{rxn}, is the difference in formation energies between the products and the reactants:

$$\Delta G_{rxn} = \Sigma\, G_{f,prod} - \Sigma\, G_{f,react}$$

Each Gibbs free energy value in ΔG_{rxn} is multiplied by the leading coefficient from the balanced chemical equation, so that is has the form:

$$\Delta G_{rxn} = cG_{f,C} + dG_{f,D} - aG_{f,A} - bG_{f,B}$$

It should be noted that the value ΔG_{rxn} represents the energy change if the chemical reaction is allowed to reach thermodynamic equilibrium. Under non-equilibrium conditions the change in Gibbs free energy is given by:

$$\Delta G = \Delta G_{rxn} + RT\ln(Q)$$

R is the gas constant from the ideal gas law and Q is the reaction quotient. The quotient Q for the sample reaction is:

$$Q = \frac{[C]^c[D]^d}{[A]^a[B]^b}$$

The brackets signify the partial pressure of the species if in the gas phase or the activity of the material if in solid phase.

The expression for the reaction quotient is identical in form to the equilibrium constant K. The difference is that K uses the concentrations of the species at thermodynamic equilibrium whereas Q uses initial values or values before equilibrium is reached. In general the constant K should be greater than unity to favor the formation of products in the reaction. Small values of K lead to low efficiency of the chemical reaction. If Q<K then the formation of more products is favored and the reaction will proceed to the right. If Q>K then the reactant species are more favored and the reaction proceeds to the left. Most film growth techniques are non-equilibrium processes, which means that the reaction quotient Q is more thermodynamically relevant than K. All thermodynamic data used for the calculations in this chapter were taken from Ref. 48.

4.2 Stability of Reactants

As mentioned in Chapter 2, ammonia thermally decomposes into hydrogen and nitrogen. At a typical GaN growth temperature of 1300K the equilibrium constant K for the decomposition reaction is approximately 8.0×10^3 with $\Delta G= -97.1$ kJ/mol. Thus almost no uncracked NH_3 exists at equilibrium at GaN growth temperatures. However, equilibrium is rarely achieved in many of the growth processes used. This is very desirable because, once nitrogen molecules have been formed, the nitrogen atoms are too tightly bound to contribute to epitaxy. In an open-flow system at atmospheric pressure only about 10% of the NH_3 dissociates [41]. This value is very system dependent and can be altered by catalytic effects from the materials in the reactor or from the reactor wall itself [49].

The interaction of gallium trichloride with hydrogen is an important consideration in GaN deposition. At 1300K the reaction

$$GaCl_{3(g)} + H_{2(g)} \Rightarrow GaCl_{(g)} + 2HCl_{(g)}$$
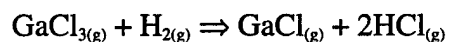
is thermodynamically favored because the Gibbs free energy change is -18.0 kJ/mol and the equilibrium constant is 5.27. Unlike ammonia decomposition, this reaction does occur to a significant degree at GaN growth temperatures [41]. Since GaCl can also be used to deposit GaN, the local (carrier) gas environment can have an effect on the growth chemistry.

The reduction of $AlCl_3$ to AlCl should also be considered for AlN growth:

$$AlCl_{3(g)} + H_{2(g)} \Rightarrow AlCl_{(g)} + 2HCl_{(g)}$$
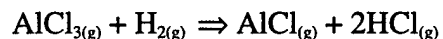
For this reaction at a typical AlN growth temperature of 1400K, $\Delta G=141$ kJ/mol and $K=5.3 \times 10^{-6}$. Therefore the reduction of aluminum trichloride in hydrogen is highly unlikely, resulting in simplified growth chemistry for AlN.

4.3 GaN Growth

When employing $GaCl_3$ as a gallium precursor for GaN growth there are two potential reactions to consider:

$$GaCl_{(g)} + NH_{3(g)} \Rightarrow GaN_{(s)} + H_{2(g)} + HCl_{(g)} \quad (1)$$
$$GaCl_{3(g)} + NH_{3(g)} \Rightarrow GaN_{(s)} + 3HCl_{(g)} \quad (2)$$
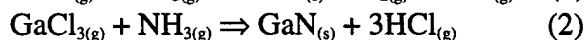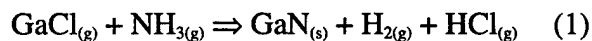
Reaction 1 is obviously important if hydrogen gas is used directly in the growth environment, but it must still be considered in the absence of intentional hydrogen because of the H_2 created by the

decomposition of ammonia. Reaction 2 is simply direct growth of GaN from the initial reactants. The list below defines parameters that are used in the reaction quotient calculations for GaN growth:

$\alpha \equiv$ fraction of NH_3 decomposed

$\gamma \equiv$ fraction of $GaCl_3$ reduced to GaCl

$a_0 \equiv$ input partial pressure of NH_3

$b_0 \equiv$ input partial pressure of H_2

$c_0 \equiv$ input partial pressure of N_2

$d_0 \equiv$ input partial pressure of $GaCl_3$

Reaction 1 has an equilibrium constant $K_1=0.557$ and free energy change $\Delta G_{rxn,1}=6.3$ kJ/mol at 1300K. The reaction quotient Q assuming unity activity for solid GaN and the corresponding Gibbs free energy change are:

$$Q_1 = \frac{[H_2][HCl]}{[GaCl][NH_3]} = \frac{2b_0 + 3\alpha a_0 - 2\gamma d_0}{a_0(1-\alpha)}$$

$$\Delta G_1 = 6.3 \text{ kJ/mol} + (10.8 \text{ kJ/mol})\ln Q$$

Reaction 2 has an equilibrium constant $K_2=2.94$ and free energy change $\Delta G_{rxn,2}=-11.7$ kJ/mol at 1300K. The reaction quotient and Gibbs free energy are:

$$Q_2 = \frac{[HCl]^3}{[GaCl_3][NH_3]} = \frac{8\gamma^3 d_0^2}{a_0(1-\alpha)(1-\gamma)}$$

$$\Delta G_2 = -11.7 \text{ kJ/mol} + (10.8 \text{ kJ/mol})\ln Q$$

Table 4.1 summarizes the results from calculations of Q_1, Q_2, ΔG_1, and ΔG_2 under a variety of gas flow rates and values of α and γ.

Reaction 1 shows a very weak dependence on the $GaCl_3$ decomposition γ for fixed $\square$. The two most important thermodynamic factors for this reaction are clearly the ammonia decomposition $\square$ and the carrier gas used. For nitrogen carrier gas, ΔG has a zero near $\square=0.16$ as is negative only when $\square$ is less than this value. Thus GaN deposition from GaCl is only favored under conditions where the ammonia is largely intact. Under an H_2 ambient, growth from the monochloride is not favored since ΔG is positive for all reasonable flow parameters. With the ammonia fixed at 1.0 slm, ΔG becomes negative only when the H_2 flow is less than 150 sccm, which is too low to be considered a true carrier flow. Without the direct addition of hydrogen, the only path for $GaCl_3$ to reduce to GaCl is through interaction with the hydrogen liberated by the ammonia decomposition reaction.

From the values in the table it can easily be seen that deposition via Reaction 2 is thermodynamically favorable for a wide range of parameters. While the size of ΔG gets smaller with increasing $\square$, it is still negative even at $\alpha=0.99$. Of course at this extreme value there is almost no active nitrogen getting to the sample surface, so very little actual deposition can occur. The same is true about the effect of γ on growth. If γ is near unity then deposition via Reaction 2 can't physically occur because there is almost no $GaCl_3$. Even though Q does not depend on the type of carrier gas, the strength of $GaCl_3$ reduction in the presence of hydrogen means that the growth rate in Reaction 2 can be adversely affected if H_2 and $GaCl_3$ are given the opportunity to interact.

The preceding calculations are only a rough estimate of the thermodynamics involved since at least one important factor has been omitted. The discrepancy is that the partial pressures used do not represent the gas composition at the substrate. While the decomposition of ammonia and the chloride in route to the sample were mostly accounted for, the creation of HCl by the deposition process was not. Since Q_1 depends directly on P_{HCl} and Q_2 on $(P_{HCl})^3$, the Q values given in the table are certainly too low. This in turn makes the ΔG values more negative than they would be in the substrate environment.

4.4 AlN Growth

When employing $AlCl_3$ for AlN growth there is only one reaction to consider:

$$AlCl_{3(g)} + NH_{3(g)} \Rightarrow AlN_{(s)} + 3HCl_{(g)}$$
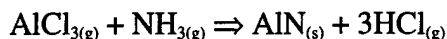
The equilibrium constant is K=678 and the free energy is ΔG_{rxn}= -75.9 kJ/mol. For the steady state reaction the appropriate quantities are:

$$Q = \frac{[HCl]^3}{[AlCl_3][NH_3]} = \frac{8\gamma^3 d_0^2}{a_0(1-\alpha)}$$

$$\Delta G = \text{-75.9 kJ/mol} + (10.8 \text{ kJ/mol})\ln Q$$

α, a_0, b_0, c_0, and d_0 are defined the same as for the GaN growth. Note that the carrier gas used in the growth is irrelevant to Q and thus will not affect the reaction chemistry. Since $AlCl_3$ does not decompose to create HCl (and the creation of HCl by the AlN growth reaction is not taken into account), the value of Q for this reaction is always equal to zero and thus independent of the growth conditions. While Q can certainly be zero before any deposition occurs (and would be indicative of an infinite driving force for the growth reaction), it is unphysical for Q to be non-zero in the steady state growth environment. Thus the first-order modeling presented for GaN growth breaks down when applied to AlN.

Based on the thermodynamic values presented, a few qualitative statements can be made about the AlN deposition reaction. The partial pressure of NH_3 will be much greater than either P_{HCl} or P_{AlCl3} since the ratio of group V to group III materials is typically in the 100s. As a result Q is always less than 1 which means that G will stay negative under almost any growth conditions. Therefore the deposition of AlN is thermodynamically favorable for any reasonable choice of gas flow parameters.

5. Results and Discussion

5.1 Introduction

All layers presented in this work were grown in the same SVPE reactor under varying gas flow conditions. The purpose of these experiments was to develop optimized parameters for the growth of thick GaN and AlN layers with good surface morphology, uniform thickness, and excellent optical and structural properties. The experimental parameters included ammonia flow, ammonia carrier flow, chloride carrier flow, chamber carrier flow, substrate temperature, chloride source temperature, substrate rotation, and chamber pressure. An equally important variable in this investigation involved the effect of the gas inlet geometry on the film quality and deposition uniformity. Many different schemes were employed to deliver the gases from the top of the reactor into the substrate region of the chamber. The two most effective methods in regards to material quality and sample uniformity were the "showerhead" discrete input and the uniform mixed input.

5.2 Gas Inlet Geometry

5.2.1 Showerhead Injector

One of the most successful methods of injecting the ammonia, ammonia carrier, and chloride carrier gases used a fixture that resembled a showerhead. The goal of this design was to keep the group III precursors separate from the group V precursors to prevent gas-phase reactions while also spreading out the reactants to improve uniformity over the 2" wafer. The upper part of the injector (Figure 5.1a) channeled $GaCl_3$ into four 2" long by 0.25" diameter tubes equally spaced along a 1.75" diameter circle. Four identical tubes on the same circle were used to inject $AlCl_3$. Ammonia was injected horizontally out of two nozzles located along the same circle as the chloride input tubes. This upper injector was made out of stainless steel.

The lower injector module (Figure 5.1b) fit around the upper piece and served two functions. First, it directed the ammonia and carrier flow vertically towards the substrate through 0.75" long by 0.188" diameter holes. One version of the showerhead had 12 holes: 4 on a 1" diameter circle and 8 on a 2" circle. A second version had 16 holes: 8 on a 1" diameter circle and 8 on a 1.5" circle. Both versions also had 8 holes to allow the passage of the injector tubes for the chlorides. The second function of this piece was to heat the stainless steel chloride input tubes and the region at the top of the chamber to prevent condensation of chloride material or of ammonia-chloride complexes. The energy was supplied by a 100W cartridge heater whose housing extended into the chamber and also into the lower injector module. In order to spread the heat more effectively than stainless steel, the lower module was constructed out of Monel because of its higher thermal conductivity.

5.2.2 Uniform Mixing Injector

The other geometry that was most successful in film deposition was the uniform mixing injector (UMI) shown in Figure 5.2. The purpose of the UMI was to intentionally mix $GaCl_3$ and ammonia at low temperatures before being directed towards the substrate in a uniform flow. This technique was based on the fact that at low temperatures ammonia and gallium trichloride react to form complexes of the form $GaCl_3 \bullet nNH_3$ where n=1,3,5,6,14, and possibly others [45]. These complexes then decomposed at the substrate at temperatures near 1050°C to form GaN. The mixing occurred by injecting the ammonia and chloride horizontally into a 1.75" diameter circular region near the top of the UMI. The only exit for the gases was vertically downward through a #30 Monel screen wire that served to make the flow uniform over the circular region. A 0.005" wall moly tube confined the gases until they were ~1.25" from the substrate. The hope was that by mixing the ammonia and chloride a more uniform deposition over the substrate area could be realized.

5.3 GaN Growth
5.3.1 Carrier-independent Effects

The growth pressure was one of the parameters whose effect on film growth was independent of the type of carrier gas used. Experiments were performed at pressures ranging from 1 to 600 torr. Those samples grown at 500 torr and above showed no deposition after one hour. Films prepared at pressures of 100 to 200 torr exhibited low growth rates but had uniform, albeit poor, deposition morphology across the wafer. Samples grown near 50 torr had reasonable growth rates, 5 – 90 $\square$m/hr, although the deposition was less uniform in surface structure and thickness over the substrate. The uniformity continued to worsen as the pressure was dropped to 20 and 10 torr with no film growth present on the outer regions of the wafer. Experiments performed at 1 torr were uniform only near the gas inlets and the growth rates were noticeably higher due to pumping action by the chamber on the source.

The other parameter that was insensitive to the choice of carrier gas was the substrate rotation. It was found that the rotation rate in the range 20 to 1000 rpm had little effect on the quality of the deposited GaN film. The only notable affect was that the pyrometer temperature for rotation rates less than 30 rpm was significantly lower than when the rotation was above 100 rpm under otherwise similar conditions. Thus the substrate rotation provided temperature uniformity across the substrate but had no other tangible benefits. In general, a rotation rate between 200 and 600 rpm was used for GaN growth.

5.3.2 Nitrogen Carrier Gas

GaN films grown early in this research employed nitrogen as a carrier gas for the ammonia and gallium trichloride. As presented in the previous chapter, GaN deposition in a nitrogen ambient is thermodynamically favorable. Table 5.1 summarizes the parameter ranges explored and the experimentally determined conditions for the best GaN growth using N_2 as a carrier gas for the NH_3 and $GaCl_3$.

The values for the NH_3 and N_2 flow rates that lead to transparent film deposition varied widely with the injection scheme used. In general, however, films that were grown under an ammonia deficiency tended to be dark in color and composed of tiny crystallites. Those experiments performed under severe NH_3 deficiency resulted in no deposition and also the removal of part or all of the GaN buffer layer on the sapphire. This degradation was caused jointly by the decomposition of GaN at high temperatures in the absence of atomic nitrogen and by the chemical etching of the film by the chloride source material. No detrimental effects were observed when films were grown under a very ammonia rich environment. In fact, the best results were obtained with a NH_3 to N_2 ratio of 3 to 1. However, when the total flow rate ($NH_3 + N_2$) was too large, samples tended to have small particles on the surface. This suggests that the gas flow above the substrate was turbulent and led to gas-phase formation of GaN crystallites. The turbulence was likely due to the high inlet gas velocity resulting from the larger flows.

The role of the substrate temperature in GaN growth is intertwined with the ammonia flow rate. Since the temperature of the sample determines the fraction of ammonia that is cracked, the N availability for GaN deposition is governed both by the NH_3 flow rate and the substrate temperature. As a result, layers grown at a low temperatures tended to be brown and made up of small crystals, just as if they were grown under an ammonia deficiency. Samples grown between 990 and 1060°C were not drastically different which implies that a temperature near 1000°C provided sufficient cracking of NH_3 to deposit GaN at a fairly high rate.

Samples grown in the showerhead injection geometry with nitrogen carrier gas exhibited bright band edge photoluminescence, reasonable x-ray line widths, and fairly high growth rates, but had a surface morphology that was not completely two-dimensional. The photoluminescence from a 120μm thick GaN sample is shown in Figure 5.3. The room-temperature emission has a narrow linewidth of 55

meV and the peak is located at 3.416 eV. The slight shift of the bandgap energy from the reported value of 3.39 eV is likely due to strain relaxation in the thick layer. A broad deep-level emission is observed in the yellow and red portion of the spectrum centered near 680nm. For GaN films grown by MOVPE and MBE, yellow band luminescence is typically seen in samples that are doped n-type with Si as well as samples that are not intentionally doped. One model for this yellow emission involves a transition between a deep donor and a shallow acceptor state [50]. Another model proposes a transition from a shallow donor to a deep acceptor level [51].

Analysis of the films by DXRC reveals peak widths for diffraction from the (0002) planes to be typically less than 600". A peak from a 45□m thick sample having a FWHM of 306" is shown in Figure 5.4. It is not uncommon for the linewidth to vary significantly over the wafer when the surface morphology is not uniform across the sample. It should also be noted that, since these measurements are taken from diffraction from the (0002) planes, the rocking curves are only sensitive to a change in the c lattice parameter. Thus this particular measurement is blind to threading dislocations which originate at the substrate-film interface. GaN layers a few microns thick grown on sapphire tend to have anywhere from 10^8 to 10^{10} threading dislocations per square centimeter.

For those layers that are transparent and exhibit good PL, there were two dominant surface morphologies observed. The first was the hexagonal growth structure shown in Figure 5.5a, where the width at the base of the peaks varied from 50 to 400□m and gave the film surface an uneven appearance to the eye. The second surface morphology observed was the irregular terraced peak structure shown in Figure 5.5b, referred to here as "volcano" features. This type of surface also appeared uneven to the eye. As seen in the previous two figures, both surface types share similar dark features. These small irregular crystal "spires" rise above the surrounding epitaxy and are prevalent over most of the samples. In some cases, their height is 3 – 4 times the thickness of the epitaxy. The "spires" give the layers a three-dimensional texture and well as making them milky in color rather than completely transparent in regions where there is a high density of the crystals. Viewed under the SEM they appear to be composed of striated, multi-faceted crystals of GaN (Figure 5.6).The process behind the growth of the tall crystals is not known. One possible explanation is that the "spires" are seeded by small GaN crystallites formed in the gas phase at the initiation of the growth that fall down onto the surface. They then grow at a faster rate than the surrounding epitaxy. Another is that the seeding process is due to turbulence above the substrate and is a continuous process, but with only a small number of the products actually making it to the surface. The formation of the "spires" could never be completely eliminated, and this difficulty led to the use of a different carrier gas for GaN epitaxy.

5.3.3 Hydrogen Carrier Gas

Due to the non-ideal surface morphology observed with nitrogen carrier gas, experiments were performed that used hydrogen carrier gas. GaN deposition from $GaCl_3$ in an H_2 ambient is not as thermodynamically favorable compared to an N_2 ambient as discussed in the last chapter, but it can proceed via one of the previously presented reaction pathways. Table 5.2 details the parameter ranges explored and the best values determined for growth of GaN using hydrogen carrier gas for the NH_3 and $GaCl_3$ and also as a chamber purge.

The flow rate of ammonia and its carrier had a large impact on the deposition morphology and thickness uniformity. Like the case using nitrogen carrier, the optimal ratio of ammonia flow to that of its hydrogen carrier flow was found to be 3 to 1 regardless of the injection geometry used. Samples that were grown under ammonia deficiency had a dark appearance with a strong three-dimensional morphology. Those films grown in the showerhead configuration with an ammonia flow that was too high exhibited either the crystal "spire" features similar to those on samples deposited with N_2 carrier gas or a rough surface texture consisting of small, rounded islands.

A somewhat larger range of growth temperatures was explored for the hydrogen carrier gas experiments. Similar to the nitrogen experiments, temperatures near 1000°C and above provided sufficient cracking of ammonia to produce transparent layers. The layers with the best properties were deposited at temperatures between 1025 and 1060°C, depending on the geometry used. Experiments performed above 1100°C resulted in no film deposition on the substrate.

The amount of hydrogen used as a chamber purge did not have a noticeable affect on GaN deposition. The flow was injected over a large area (a ring whose inner and outer radii were 1.25" and 2.563", respectively) but was excluded from the central region over the sample by the moly shield that constrained the ammonia and chloride flows. Thus the chamber purge had little effect on the local gas environment at the substrate and, as a result, did not significantly affect the growth.

Compared to the experiments using nitrogen carrier gas, samples grown using hydrogen carrier gas in the showerhead and UMI configurations exhibited similar band edge photoluminescence, x-ray line widths, and growth rates, while having improved surface morphology. The PL from a 38μm thick GaN sample grown at 20 torr in the showerhead design is shown in Figure 5.7a. The room-temperature emission has a linewidth of 67 meV with the peak located at 3.416 eV. Unlike the layer grown with nitrogen carrier gas, the deep level emission band is centered in the yellow as opposed to red. For samples grown in the UMI geometry, the PL was slightly broader (FWHM = 71 meV) with deep level emission in the red (Figure 5.7b). Experiments in both inlet configurations tended to have a weak emission centered near 440 nm that was unexplained. Thicker samples were dominated completely by band-edge luminescence, as seen by the PL of a 300μm thick sample in Figure 5.7c.

The use of hydrogen as a carrier gas provided the best GaN x-rays in this project. Figure 5.8 shows the DXRC of a 30μm thick sample grown in the showerhead configuration with a FWHM of 274". Films grown with H_2 carrier gas typically had line-widths less than 500", and like the nitrogen growths, the FWHM values varied across the wafer.

The surface morphology of samples grown in an H_2 ambient was similar to the N_2 growth experiments in that both hexagonal and volcano features were typically observed. The difference, however, was a greatly reduced number of the crystal spire growths observed on the films. In many cases the samples with hexagonal structure exhibited smaller island features and had almost no spires present (Figure 5.9a). Those films with the volcano morphology tended to have a number of the spires present, namely in the centers of the volcano peaks (Figure 5.9b). The change from nitrogen to hydrogen carrier gas was successful in reducing the number of crystal "spire" growths on the GaN surfaces. Otherwise, the overall morphology of the deposition was not strongly affected. The switch in carrier gas did not drastically affect photoluminescence and DXRC measurements.

5.4 AlN Growth

Consistent with the thermodynamic analysis in Chapter 4, the type of carrier gas used had no noticeable affect on AlN deposition, at least at the lower end of the growth temperature range. Those experiments performed under similar conditions had identical surface morphologies, structural characteristics, and wafer uniformity. It should be noted that films grown in the higher temperature regime employed only hydrogen carrier gas.

Because fewer experiments were performed involving the growth of AlN, the parameter ranges were somewhat narrower. Typically the optimum values of the pressure, ammonia flow, and carrier flow used to grow GaN in a given geometry were used in the AlN growth experiments. The best film characteristics were obtained with the showerhead configuration. As with GaN deposition, the substrate rotation and chamber purge flows were found to have little effect on film quality and will not be discussed further. The parameter ranges explored, as well as the most successful values, are given in Table 5.3.

In other growth systems the deposition of AlN is typically performed at temperatures higher than for GaN, and the same trend was expected for SVPE. Films grown around 1000°C were transparent but hazy with a dull surface finish. Under low magnification, the film surface was generally smooth but had a high density of circular brown lumps (Figure 5.10a). An SEM scan at higher magnification reveals that a columnar growth structure was present for these layers (Figure 5.10b). As the growth temperature was increased, the AlN layers became more transparent and shiny in appearance as the dark lumps disappeared. A side effect of raising growth temperature was that the GaN buffer layers on which the AlN films were deposited tended to crack and peel. This breakdown was due to the fact that the GaN buffer was deposited at significantly lower temperature than the AlN epitaxy. At a growth temperature of 1160°C, deposition of a shiny, transparent film was possible, but with the surface appearing broken and flaky at low magnifications (Figure 5.11a). Higher magnifications reveal small, odd-shaped features that were unlike any morphology seen before in this work (Figure 5.11b). The nature of these features is unknown, but it may be speculated that they are due to the breakdown of the underlying buffer layer.

In the range of flows explored, the concentration of ammonia used had no strong effect on the quality of AlN deposition. Similar to GaN growth, however, AlN films tended to be poorer when the total ammonia plus carrier flow was too large. The films in this case tended to have duller surfaces and be less transparent. One positive result of the higher flows was better thickness uniformity across the wafer as evidenced by fewer growth rings (Newton's rings).

The AlN samples were grown at a reduced growth rate compared to the GaN. A deposition of 5 – 30μm was typical after a one-hour experiment, with the thickness different by a factor of two or three from the center to the edge. Several of the films exhibited cathodoluminescence near the band edge and had reasonable DXRC line widths.

The CL spectrum from an AlN sample grown at low temperature (1000°C) is shown in Figure 5.12a. As seen by the logarithmic scale in the graph, the near band-edge luminescence at 210.5 nm (5.891 eV) is very weak compared to the broad deep level emission bands. It is known that oxygen incorporates readily into AlN during growth and also interacts with film surfaces at room temperature to form an oxide layer. Oxygen-related CL peaks typically show up at wavelengths near 375 nm [52]. The deep level peaks observed in the low temperature AlN could therefore be oxygen-related or perhaps arise from some other defect states in the gap.

AlN grown at a temperature of 1160°C exhibits a much brighter near band-edge peak (Figure 5.12b) as shown by the linear scale on the graph. The near band-edge peak is shifted to 217 nm (5.714 eV) compared to the low-temperature AlN sample and has a strong, narrow deep level emission at 598 nm (2.074 eV). The broad luminescence between 300 and 500 nm is likely emission from oxygen impurities or surface contamination.

The best x-ray FWHM values were obtained for AlN samples grown at low temperatures. The (0002) rocking curve for a film grown at 1000°C and having a FWHM of 484" is shown in Figure 5.13a. Because of the degradation of the underlying GaN buffer layer, the x-ray linewidths for AlN layers became larger as the growth temperature was increased (Figure 5.13b). Thus the structural quality of the layers as measured by DXRC is not optimized at the same growth temperature as the optical properties.

Clearly what are needed are AlN buffer layers grown on sapphire at high temperatures to serve as templates for thicker AlN epitaxy. During the time of this work only GaN buffer layers were available to use as substrates. Several attempts were made to deposit AlN directly on sapphire but all resulted in growth of polycrystalline material.

5.5 AlGaN Growth

A small number of attempts were made to grow AlGaN using both chloride sources simultaneously. The growth conditions were chosen to be the optimized parameters for the geometry

was present. In general, deposition was hindered by gas phase reactions between $GaCl_3$ and $AlCl_3$. The formation of a complex of these chlorides, $GaCl_3 \bullet AlCl_3$, is favorable [45]. The majority of growths resulted in non-transparent material whose surfaces were rough due to the formation of small crystallites of AlGaN. In a few cases, low Al content layers were deposited transparently over large areas of the wafer. The growth parameters for two of these layers, S165 and S221, are summarized in Table 5.4.

Layer S165 was not grown in the showerhead or UMI inlet configurations. The geometry for this sample had the ammonia injected horizontally at the top of the chamber with the $GaCl_3$ and $AlCl_3$ each separately injected through a 0.25" tube, the aluminum trichloride tube being longer by 0.25". The chloride tubes were not centered on the substrate, but they were angled so that they pointed approximately 0.125" from the center of the wafer

The optical microscope image of the surface of this AlGaN sample is shown in Figure 5.14. The morphology consists of volcano features seen in the GaN growths as well as crystallites scattered about the sample. A CL spectrum taken from this sample at room temperature (Figure 5.15) exhibits emission peaks at 3.713 eV (334 nm) and 3.469 eV (357.5 nm). These values correspond to aluminum contents of 16% and 4%, respectively. Since a non-uniform alloy composition would be expected to exhibit a broad peak instead of two narrow emission bands, the spectrum may indicate segregation of the Al. CL images taken of the sample at the two peak wavelengths reveal that the luminescence has a definite spatial variation. The 334 nm emission (Figure 5.16a) occurs from the crystallites as well as from the surrounding epitaxy with the notable exception of the steps around the volcanoes. The scan of the same region at 357.5 nm is given in Figure 5.16b and shows luminescence mainly at the ledges of the volcano structures with a lack of emission elsewhere. Thus it seems that, for whatever reason, the growth ledges have a significantly lower Al content than other parts of the layer. For comparison purposes, a standard SEM image (secondary electron) of the region is given in Figure 5.16c. It is also possible that the lower energy peak represents emission from a shallow defect state similar to the 440nm luminescence observed in some GaN samples. However, the relative narrowness of the 357.5 nm peak makes this explanation less feasible.

The second sample, S221, was grown in the showerhead geometry with a modification that extended the $AlCl_3$ inlet tubes closer to the substrate to reduce any pre-reaction with $GaCl_3$. The extensions were made out of molybdenum due to their proximity to the substrate. The distance from the end of the tubes to the substrate was approximately 1.5".

The surface morphology of this layer is hexagonal with small crystallite features (Figure 5.17). The CL emission spectra is given in Figure 5.18 and contains only one band-edge peak at 358 nm (3.464eV) corresponding to an Al mole fraction of approximately 4%. A weaker luminescence centered near 410 nm is also observed. The low energy luminescence in this case is most likely the same 440 nm phenomenon seen on some GaN growths, only shifted to a higher energy. An image taken at 358 nm reveals uniform emission over the region with the exception of a network of cracks which appear (Figure 5.19a). The regions near these cracks are the strongest source of the 410 nm luminescence as shown by Figure 5.19b. No cracks are observed in the secondary electron image taken of the same region (Figure 5.19c).

The two most important factors affecting the growth of AlGaN by this method are the interaction between the chloride species and homogenizing the Al content. The most straightforward solution to the first problem would be separating the chlorides until just above the substrate to minimize the mixing and interaction time. However, it was discovered during growth of the binary materials that if the moly injection tubes were brought close to the substrate the heating of the metal promoted early chloride decomposition as well as formation of nitride material on and in the tubes.

A potential solution to the homogeneity problem would be to inject the AlCl$_3$ and GaCl$_3$ independently through a series of small holes over an area about the size of the substrate. This drawback of this design is that the injection head would need to be very close to the substrate to overcome the interaction problem and would then likely cause the same chloride decomposition and nitride deposition mentioned earlier. Thus it is not clear how to best modify the source material injection scheme in order to grow uniform AlGaN of good crystalline quality.

5.6 Additional Results

Even though the thermodynamics of GaN growth in the SVPE system are highly favorable, it is possible that other influences, like the gas dynamics and surface kinetics, are responsible for the observed sample morphologies. Typical HVPE reactors are operated near atmospheric pressure under relatively isothermal conditions compared to SVPE, and it may be due to these factors that HVPE has been more successful in depositing smoother GaN layers. The higher system pressure implies that gas residence time in the chamber is longer. Coupled with the heating of the reactor wall, this means that the gas molecules will be more energetic by the time they reach the substrate. It is very possible that the hotter gases can result in a smoother surface finish compared to the cooler injection used in the SVPE system.

To better explore the higher-pressure, hotter gas growth regime that most researchers employ for standard HVPE, a vertical hot-wall quartz reactor was recently designed and constructed. The system is comprised of a 4" diameter quartz tube which serves as the deposition chamber, a low rotation sample mount capable of holding 2" wafers, and a gated load lock for sample entry and removal that does not expose the chamber to ambient. The same pumping equipment, solid source reservoirs, and gas flow controls from the low-pressure system are used in the current reactor design (Figure 5.20, 5.21). The glass-to-metal seals are made with water-cooled o-ring connections. Reactants are delivered to the substrate in separate quartz tubes to prevent premature interaction. The single-zone furnace that heats the reactor chamber is designed to operate at temperatures up to 1300°C and is manufactured by International Thermoproducts.

All experiments performed to date have been deposition of GaN onto sapphire substrates with a GaN buffer pre-deposited by MOVPE. A pressure of 700 torr was used for the growths, which lasted one hour. Only ammonia and nitrogen gases were employed — no hydrogen was used. The other experimental parameters were as follows: ammonia 0.7–3.5 slm, nitrogen chamber flow 0–2.5 slm, GaCl$_3$ carrier flow 300–800 sccm at 70–125°C source temperature, and furnace temperature of 975–1065°C. Substrates were rotated at 30 rpm for the duration of the experiment.

Samples grown near atmospheric pressure in the hot-wall reactor tended to be transparent with a shiny surface finish. Layers were grown that had neither the "volcano" nor the hexagonal features seen with the previous reactor design (Figure 5.22). These surfaces do have some degree of three-dimensionality, but overall are smoother than their counterparts from the cold-wall system. Thus, it seems that the current hot-wall SVPE design is capable of depositing GaN films with better surface morphology than the previous reactor.

6. Conclusions

It has been demonstrated in this work that thick GaN with good optical properties and DXRC measurements can by deposited at MOVPE pressures by SVPE using gallium trichloride and ammonia. The number of crystal "spires" of the surface of the samples was greatly reduced by using hydrogen as a carrier gas in place of nitrogen. However, in order to use thick SVPE GaN films as substrates ("quasi-bulk") for device structures, a flat and uniform surface devoid of hexagons and "volcanoes" is necessary. Efforts to smooth the surface morphology in the cold-wall reactor by varying the growth conditions were not entirely successful. Growths performed in a hot-walled quartz reactor, however, showed marked improvement in the smoothness of the samples. Thus, the preliminary results indicate that the isothermal, near atmospheric-pressure growth environment is critical to obtaining smooth GaN sample surfaces when employing $GaCl_3$ and NH_3 as reactants. Further improvement of the GaN growth morphology should be possible with the optimization of the experimental conditions.

The growth of thick AlN by SVPE showed promise as evidenced by the near-band edge cathodoluminescence and the generally smooth surface. Breakdown of the underlying buffer layer could be remedied by the use of AlN instead of GaN. Hopefully this would eliminate the small blocky crystals and ring-shaped features from the surface of the films. AlN buffer layers would also allow exploration of higher growth temperatures which could lead to better optical and structural properties.

Experiments regarding the deposition of AlGaN by $GaCl_3$ and $AlCl_3$ showed promise. Incorporation of small aluminum mole fractions was demonstrated with films having surface features similar to the GaN layers grown in this work. The chief problems of chloride interaction and sample uniformity remain to be solved. An injection scheme to prevent chloride mixing while distributing the materials uniformly over the wafer still needs to be developed. If this problem can be addressed, SVPE could prove to be a viable method for thick AlGaN fabrication.

Tables

Table 2.1. Properties of III-N Semiconductors and Selected Substrates

Material	Lattice Constant (Å)	Band Gap Energy (eV)	Thermal Conductivity (W/cm*K)	Thermal Expansion (x10⁻⁶K⁻¹)
GaN	a=3.1892 c=5.1850	3.39 (300K) 3.50 (1.6K)	1.3	a: 5.59 c: 3.17
AlN	a=3.112 c=4.980	6.2 (300K) 6.28 (5K)	2.0	a: 4.2 c: 5.3
InN	a=3.548 c=5.760	1.89 (300K)		a: 5.7 c: 3.7
Al₂O₃ (c-plane)	a=4.758 c=12.991	8.4 (300K)	0.5	a: 7.5 c: 8.5
SiC (6H)	a=3.08 c=15.12	2.86 (300K)	4.9	a: 4.2 c: 4.7
ZnO	a=3.249 c=5.205	3.20 (300K) 3.44 (4.2K)	0.54	a: 4.8 c: 2.9

Table 4.1 Results of Thermodynamic Calculations for GaN Growth

NH$_3$ Decomp. α	GaCl$_3$ Decomp. γ	NH$_3$ flow (slm)	H$_2$ flow (slm)	N$_2$ flow (slm)	GaCl$_3$ flow (slm)	Q1	Δ G1 (kJ/mol)	Q2	Δ G2 (kJ/mol)
0.1	0.99	1	0	2	0.005	0.32	-5.94	0.02	-53.17
0.1	0.99	1	2	0	0.005	4.77	23.18	0.02	-53.17
0.1	0.5	1	0	2	0.005	0.33	-5.76	5.56E-05	-117.61
0.1	0.5	1	2	0	0.005	4.77	23.19	5.56E-05	-117.61
0.1	0.1	1	0	2	0.005	0.33	-5.61	2.47E-07	-176.15
0.1	0.1	1	2	0	0.005	4.78	23.20	2.47E-07	-176.15
0.5	0.99	1	0	2	0.005	2.98	18.10	0.04	-46.82
0.5	0.99	1	2	0	0.005	10.98	32.20	0.04	-46.82
0.5	0.5	1	0	2	0.005	2.99	18.14	1.00E-04	-111.25
0.5	0.5	1	2	0	0.005	10.99	32.21	1.00E-04	-111.25
0.5	0.1	1	0	2	0.005	3.00	18.17	4.44E-07	-169.80
0.5	0.1	1	2	0	0.005	11.00	32.22	4.44E-07	-169.80
0.9	0.99	1	0	2	0.005	26.90	41.88	0.19	-29.42
0.9	0.99	1	2	0	0.005	66.90	51.73	0.19	-29.42
0.9	0.5	1	0	2	0.005	26.95	41.90	5.00E-04	-93.86
0.9	0.5	1	2	0	0.005	66.95	51.74	5.00E-04	-93.86
0.9	0.1	1	0	2	0.005	26.99	41.92	2.22E-06	-152.40
0.9	0.1	1	2	0	0.005	66.99	51.75	2.22E-06	-152.40

Table 5.1 GaN Growth Conditions Using Nitrogen Carrier Gas

Experimental Parameter	Range Explored	Value for Best Results
Pressure	1 - 500 torr	50 torr
Substrate Temperature	900 - 1060°C	990°C
NH_3 Flow	0.2 - 5.0 slm	3.0 slm
NH_3 Carrier Flow	0.0 - 5.0 slm	1.0 slm
$GaCl_3$ Temperature	40 - 140°C	85°C
$GaCl_3$ Carrier Flow	0 - 800 sccm	300 sccm

Table 5.2 GaN Growth Conditions Using Hydrogen Carrier Gas

Experimental Parameter	Range Explored	Value for Best Results (Showerhead)	Value for Best Results (UMI)
Pressure	10 - 600 torr	50 torr	50 torr
Substrate Temperature	980 - 1130°C	1060°C	1025°C
NH_3 Flow	1.0 - 9.0 slm	4.5 slm	3.0 slm
NH_3 Carrier Flow	0.5 - 10.0 slm	1.5 slm	1.0 slm
$GaCl_3$ Temperature	70 - 130°C	85°C	85°C
$GaCl_3$ Carrier Flow	300 - 1000 sccm	500 sccm	800 sccm
Chamber Purge Flow	0.0 - 12.0 slm	4.0 slm	4.0 slm

Table 5.3 AlN Growth Conditions

Experimental Parameter	Range Explored	Value for Best Results
Pressure	50 torr	50 torr
Substrate Temperature	1000 - 1160°C	1160°C
NH_3 Flow	2.0 - 9.0 slm	4.5 slm
NH_3 Carrier Flow	1.0 - 4.0 slm	1.5 slm
$AlCl_3$ Temperature	90 - 150°C	130°C
$AlCl_3$ Carrier Flow	150 - 700 sccm	700 sccm

Table 5.4 AlGaN Growth Conditions

Experimental Parameter	Seperate Tube Injection (N₂ Carrier)	Showerhead Injection (H₂ Carrier)
Pressure	50 torr	50 torr
Substrate Temperature	970ºC	1060ºC
NH₃ Flow	4.0 slm	4.5 slm
NH₃ Carrier Flow	4.0 slm	1.5 slm
GaCl₃ Temperature	85ºC	85ºC
GaCl₃ Carrier Flow	400 sccm	500 sccm
AlCl₃ Temperature	130ºC	130ºC
AlCl₃ Carrier Flow	300 sccm	600 sccm

Figures
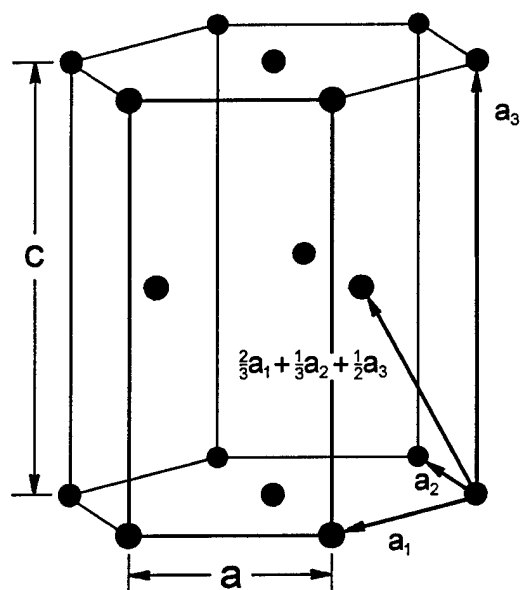
Figure 2.1 The Hexagonal Close-Packed (HCP) Structure (from Ref. 8)
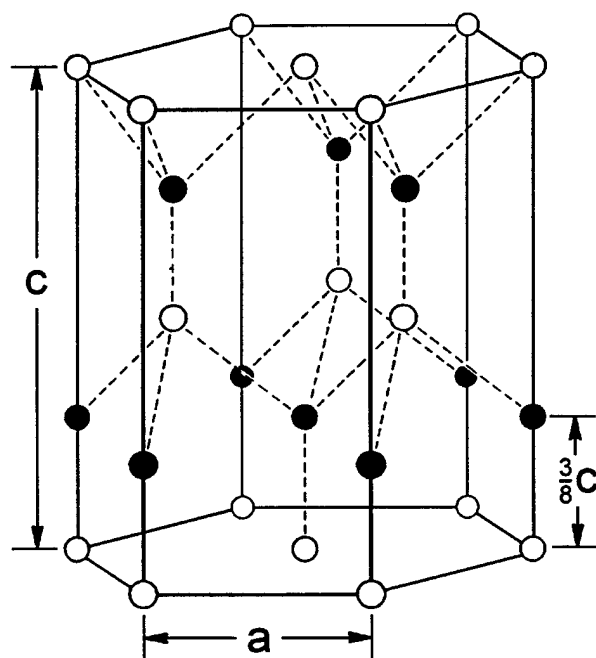
Figure 2.2 The Wurtzite Structure (from Ref. 8)
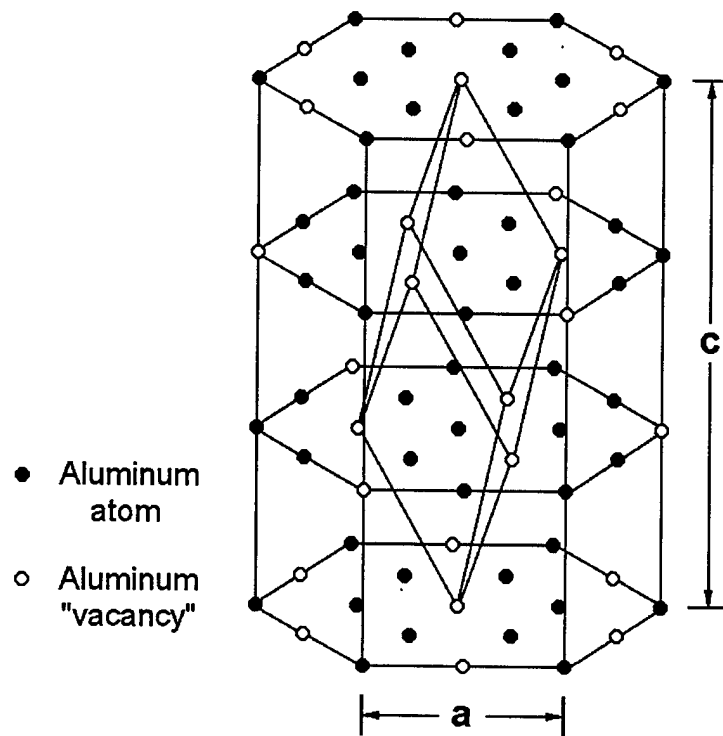
Figure 2.3 Sapphire Unit Cell Showing Al Atomic Positions. The primitive (rhombohedral) cell is shown in the interior. The conventional (hexagonal-based) cell is depicted with the lattice parameters a and c. Positions of the oxygen atoms are not shown (from Ref. 28).
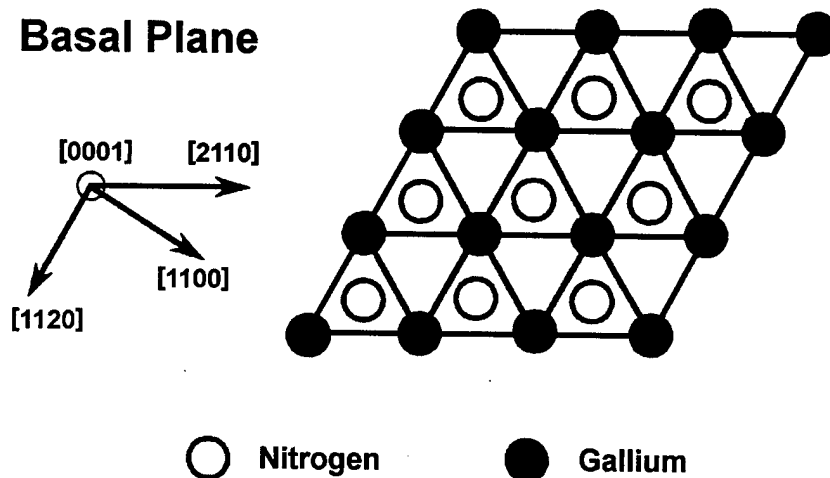
Figure 2.4 The Top View of the Wurtzite Structure (from Ref. 28)
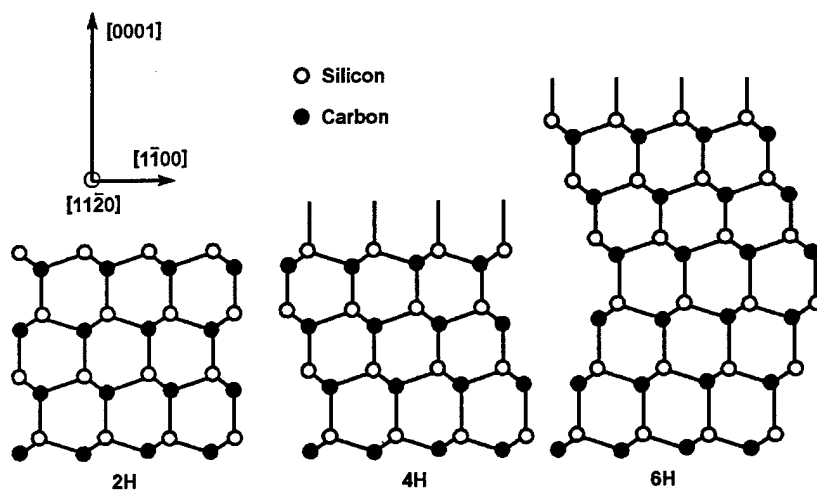
Figure 2.5 Stacking Sequence of Common SiC Polytypes (from Ref. 28)
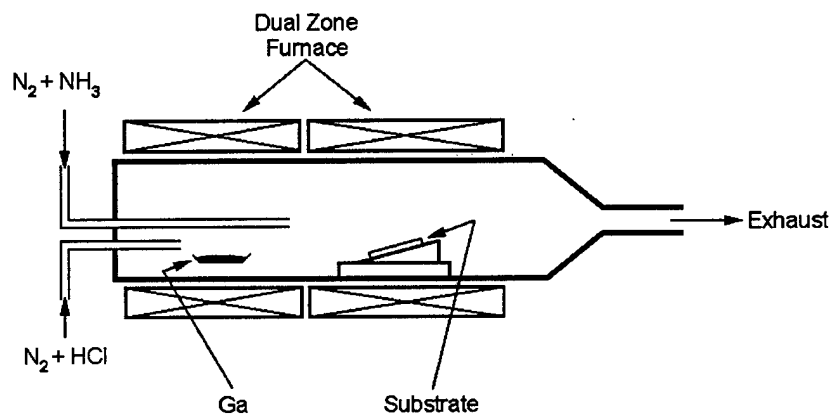
Figure 2.6 Typical Horizontal HVPE Reactor
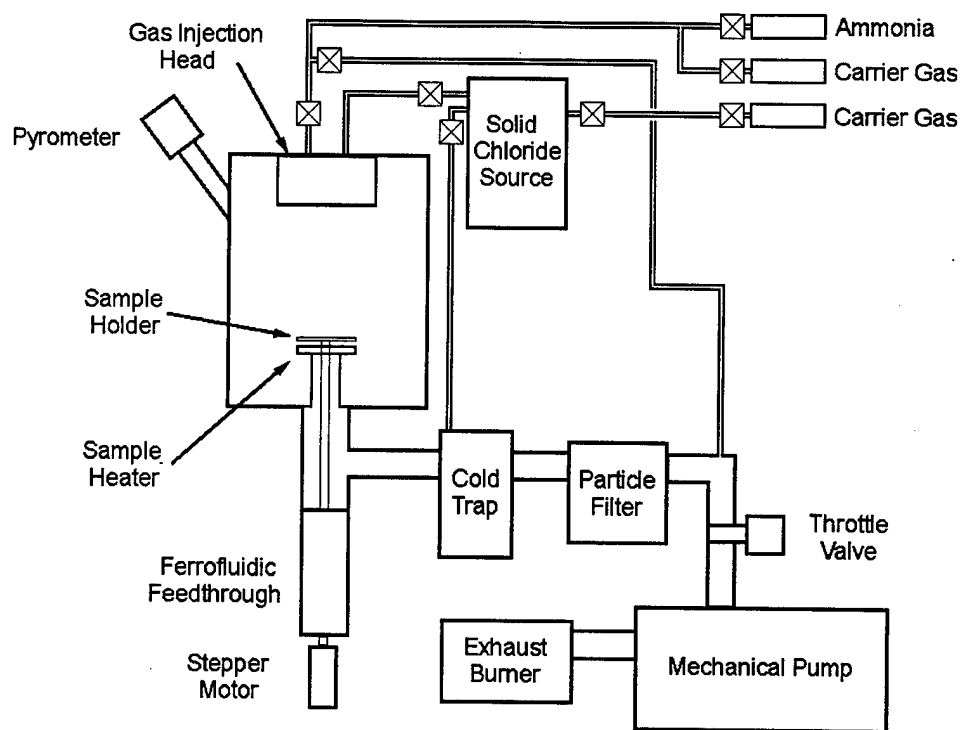
Figure 3.1 Schematic of the SVPE Growth Chamber and Related Equipment
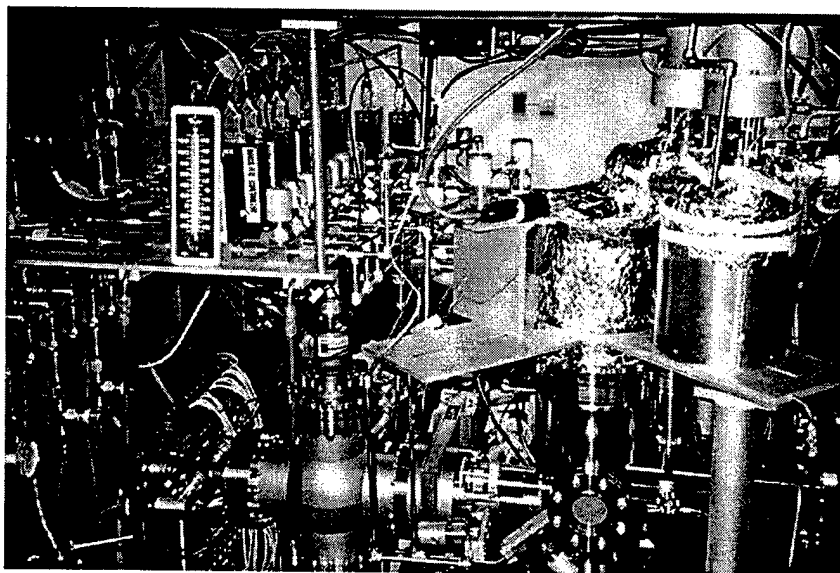
Figure 3.2 Side View of SVPE Crystal Growth System. The chloride sublimation sources are near the top right of the picture with the main chamber just below and to the left.
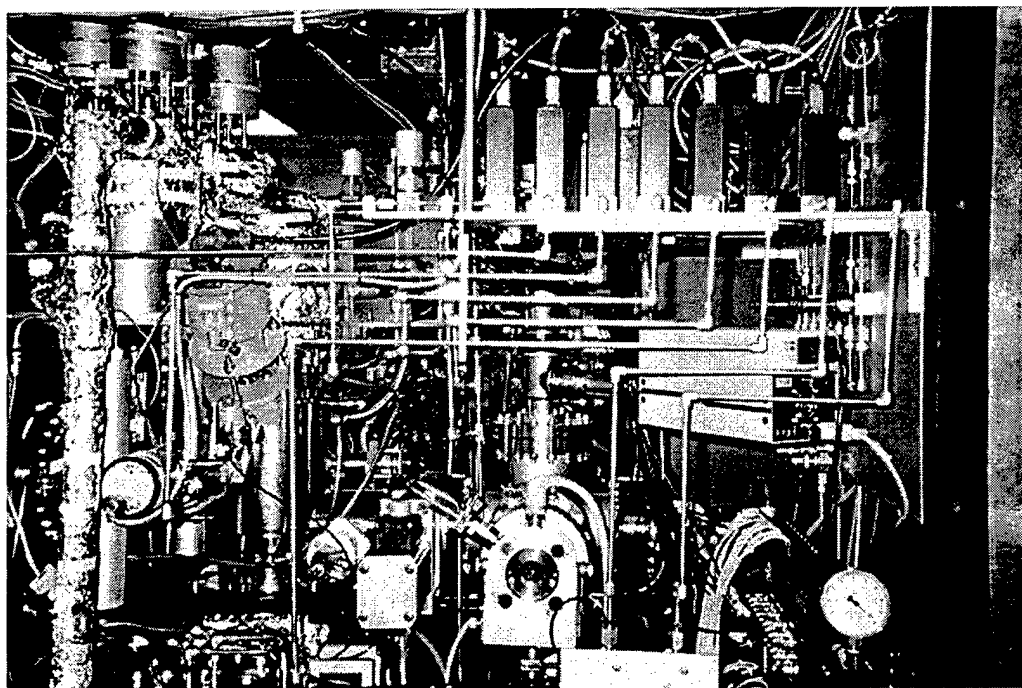
Figure 3.3 Reverse View of SVPE Crystal Growth System.
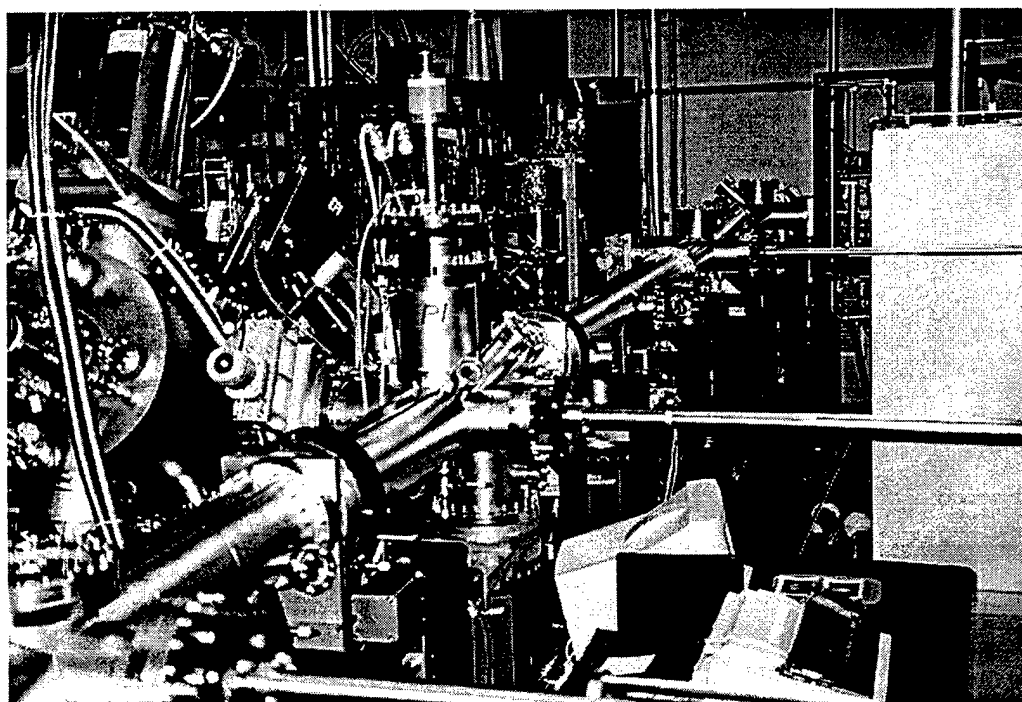
Figure 3.4 NCSU Nitride "Cluster Tool". The features include MBE,
bulk crystal growth by SVPE, and MOVPE.
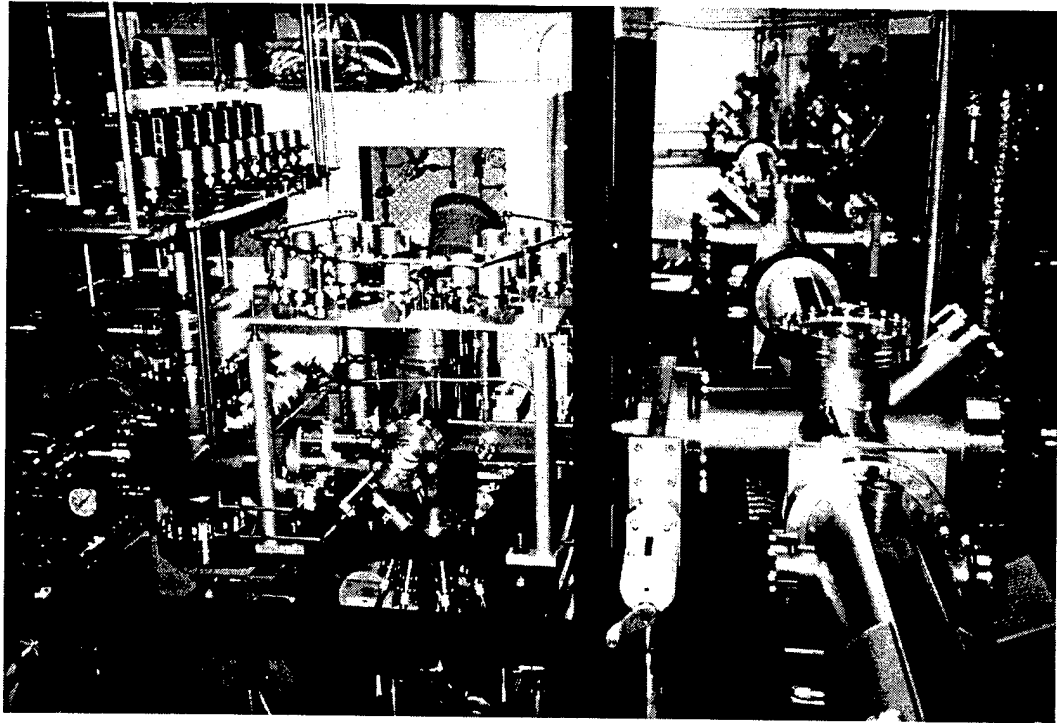
Figure 3.5 Nitride MOVPE Deposition
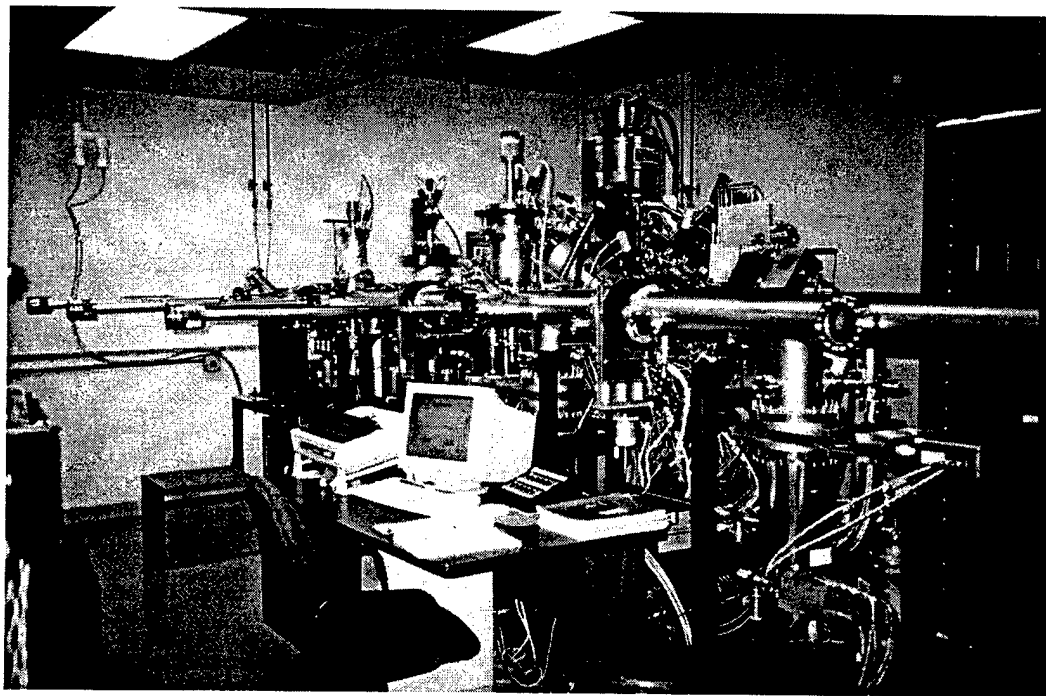
Figure 3.6 Nitride Molecular Beam Epitaxy System
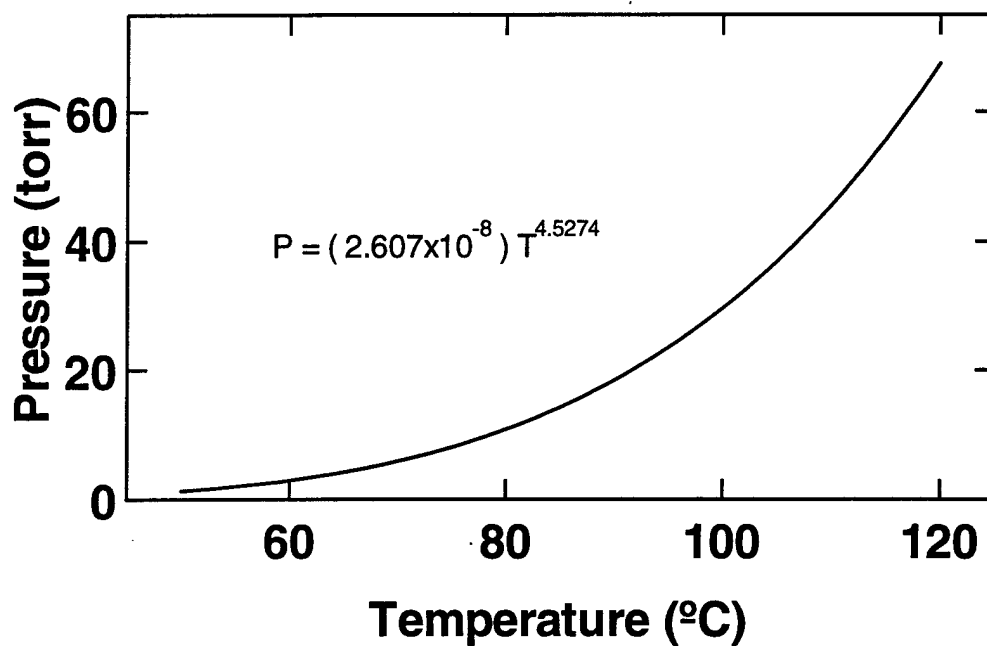
Figure 3.7 Vapor Pressure versus Temperature for GaCl$_3$
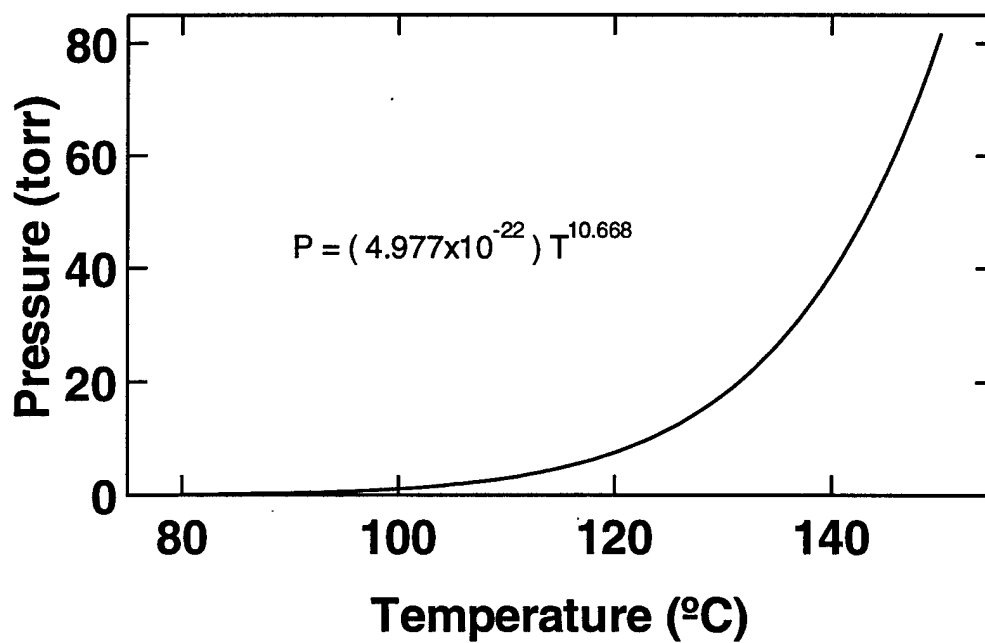
Figure 3.8 Vapor Pressure versus Temperature for AlCl$_3$
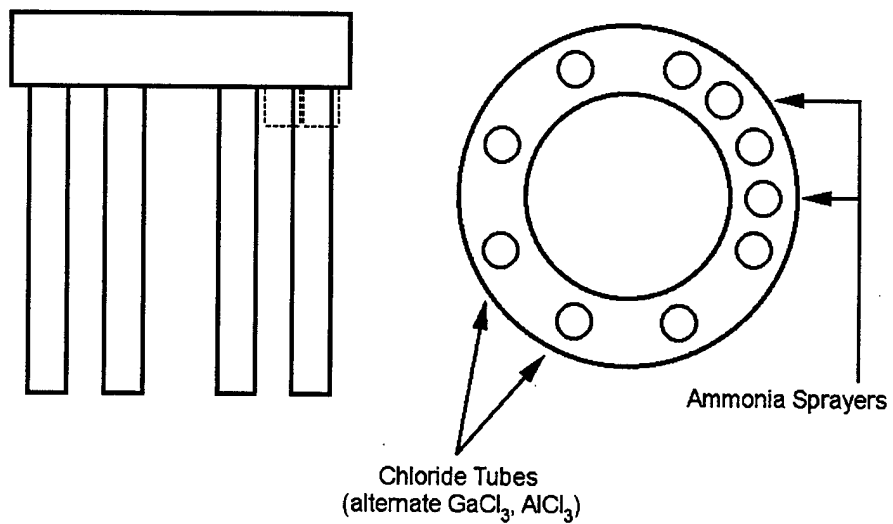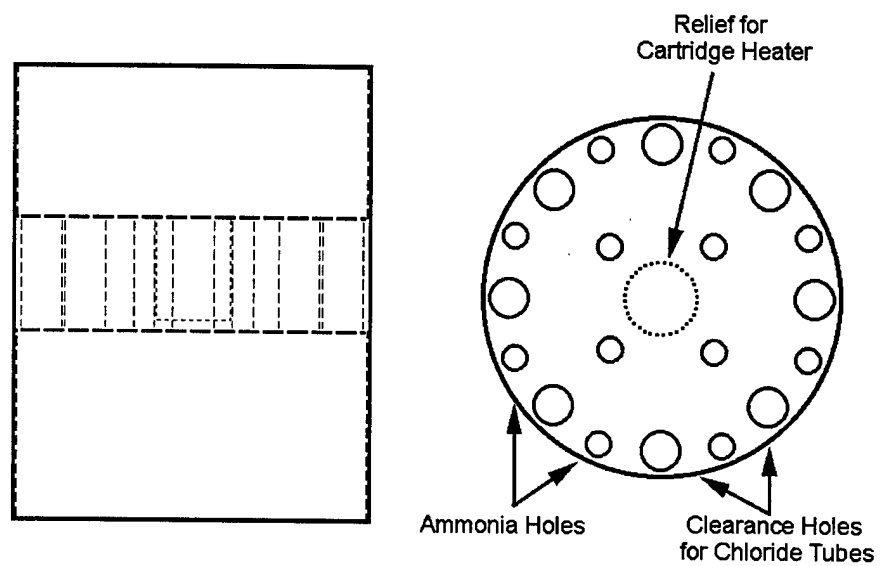
Figure 5.1a Top of Showerhead Injector

Figure 5.1b Bottom of Showerhead Injector

Ammonia Sprayers

Chloride Tubes
(alternate $GaCl_3$, $AlCl_3$)

ıia Sprayers

Chloride Tubes
(alternate $GaCl_3$, $AlCl_3$)

Figure 5.1a Top of Showerhead Injector

Reliof for

Relief for
Cartridge Heater

Ammonia Holes

Clearance Holes
for Chloride Tubes

Figure 5.1b Bottom of Showerhead Injector

heated Monel
body

tubes for AlCl$_3$ screen wire

moly
confinement

gas distribution
channels
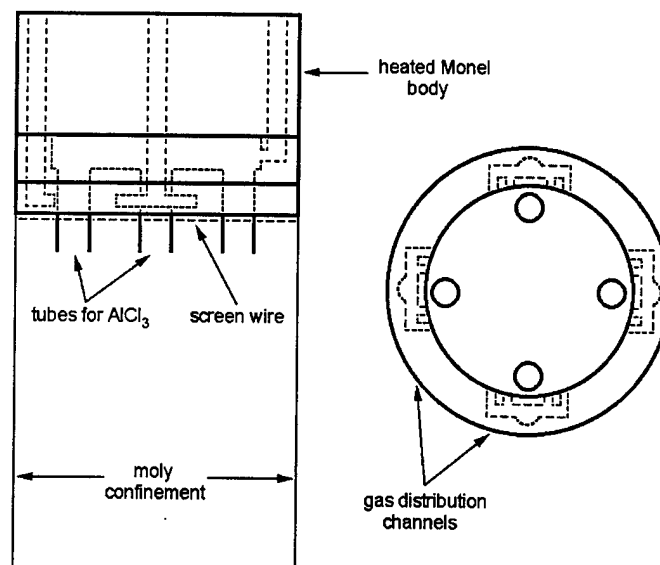
Figure 5.2 Uniform Mixing Injector (UMI)

363.0 nm
(3.416 eV)

FWHM = 5.85 nm (55.0 meV)

(S178)
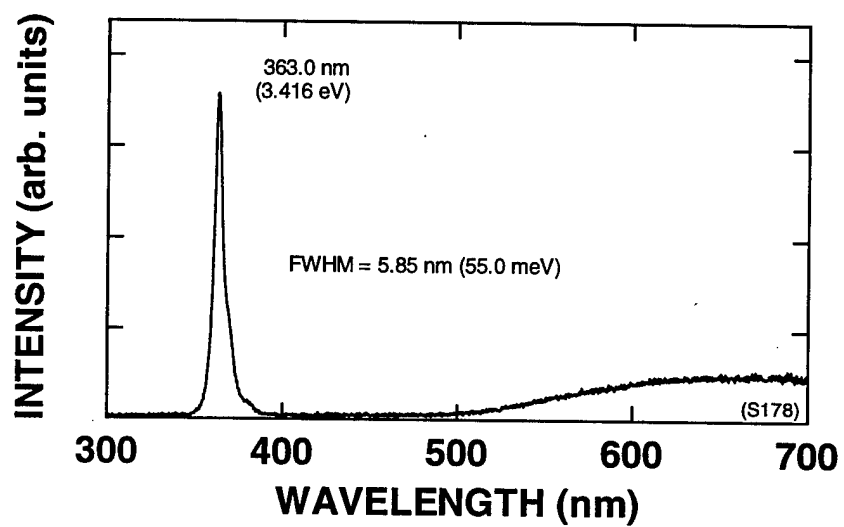
Figure 5.3 Room Temperature Band Edge Photoluminescence of GaN
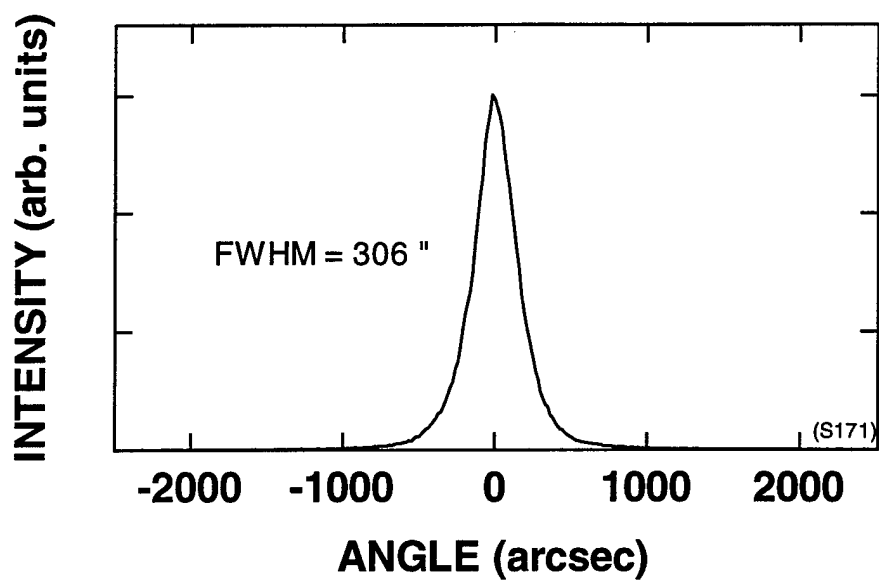
Figure 5.4 X-ray Rocking Curve of GaN
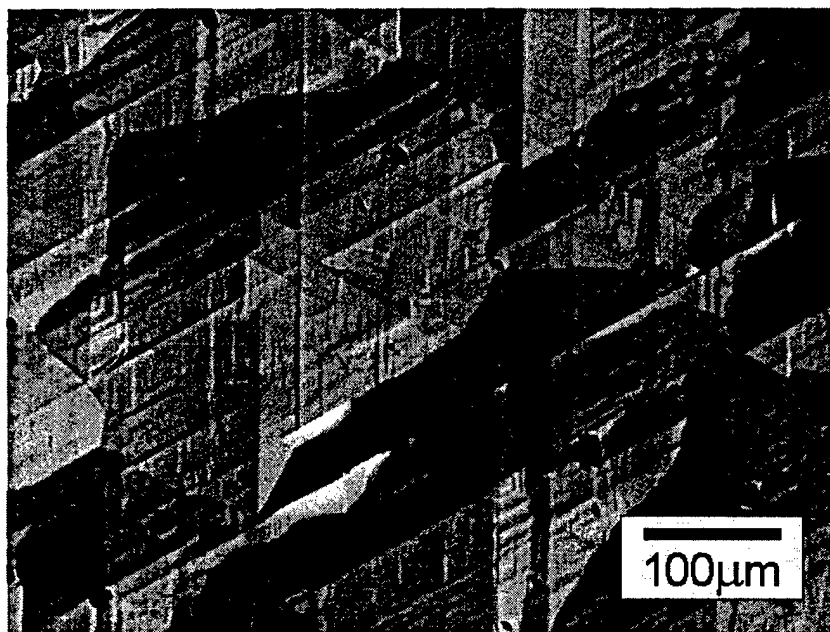
Figure 5.5a Hexagonal Morphology of GaN. This sample was grown with nitrogen carrier gas.
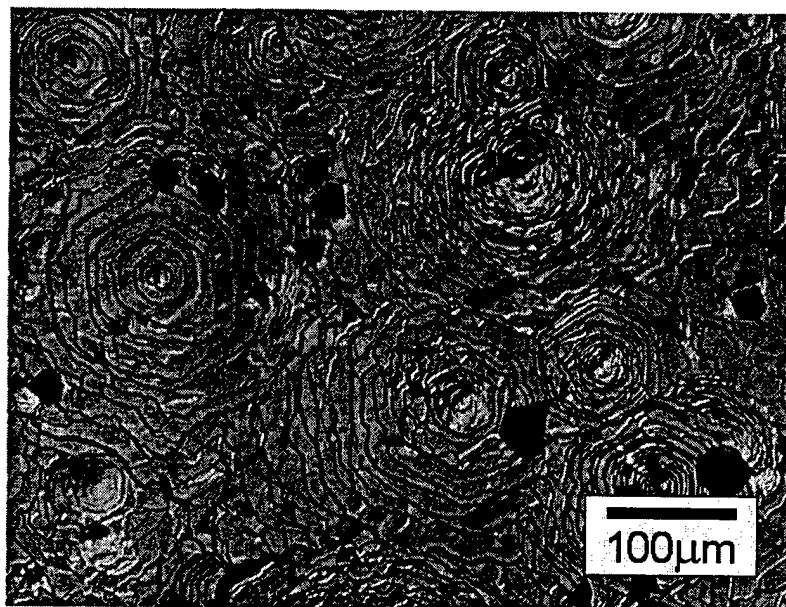
Figure 5.5b "Volcano" Morphology of GaN. This sample was also grown using nitrogen carrier gas.
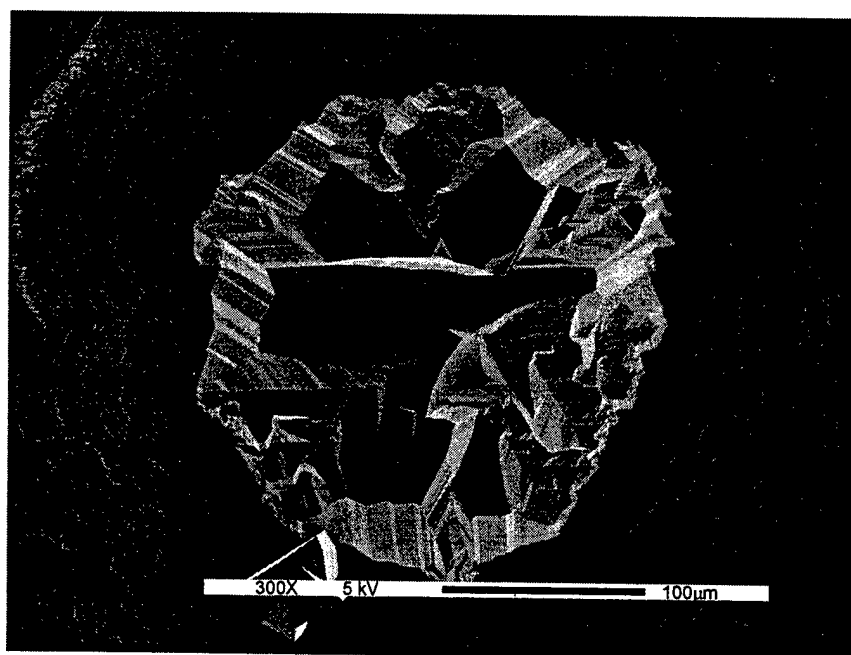
Figure 5.6 SEM Image of Crystal Spire

363.0 nm
(3.416 eV)

FWHM = 7.2 nm (67 meV)

(S217)
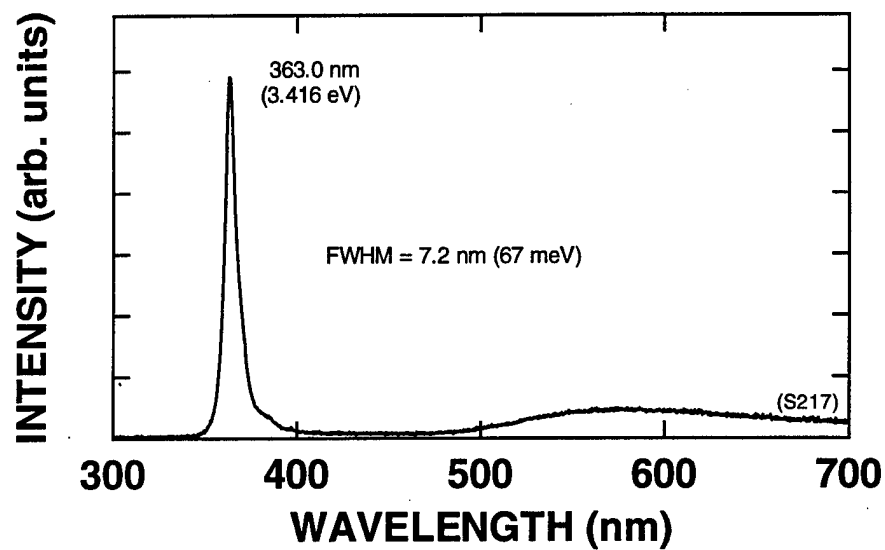
Figure 5.7a PL from GaN Grown in the Showerhead Configuration

362.0 nm
(3.425 eV)

FWHM = 7.5 nm (71 meV)

(S264)
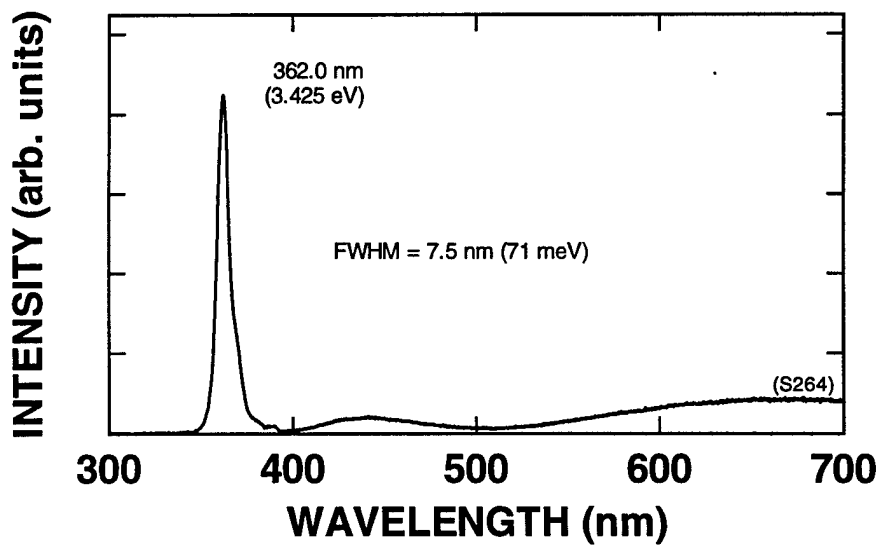
Figure 5.7b PL from GaN Grown in the UMI Configuration
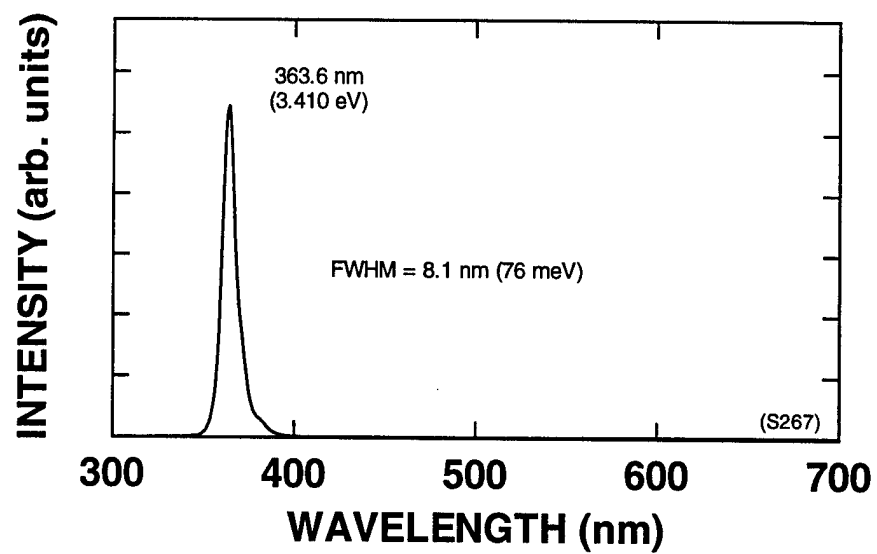
Figure 5.7c PL from 300μm Thick GaN
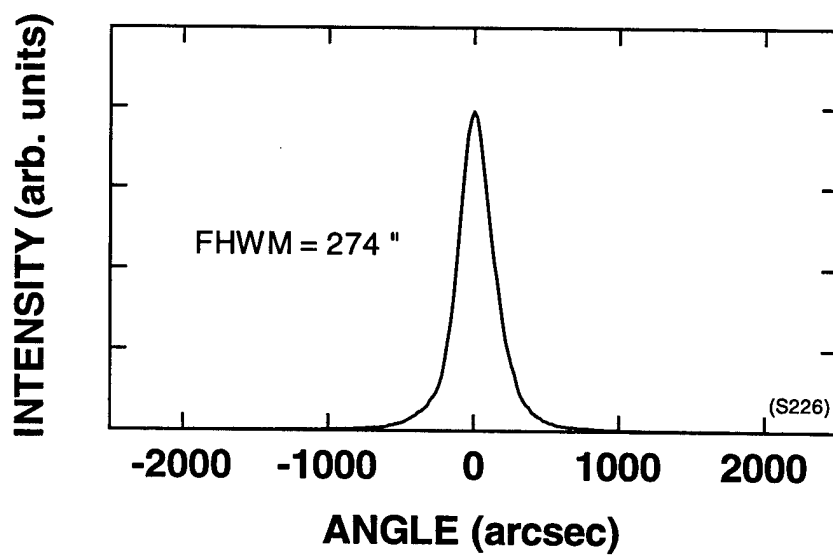
Figure 5.8 Narrow DXRC from GaN
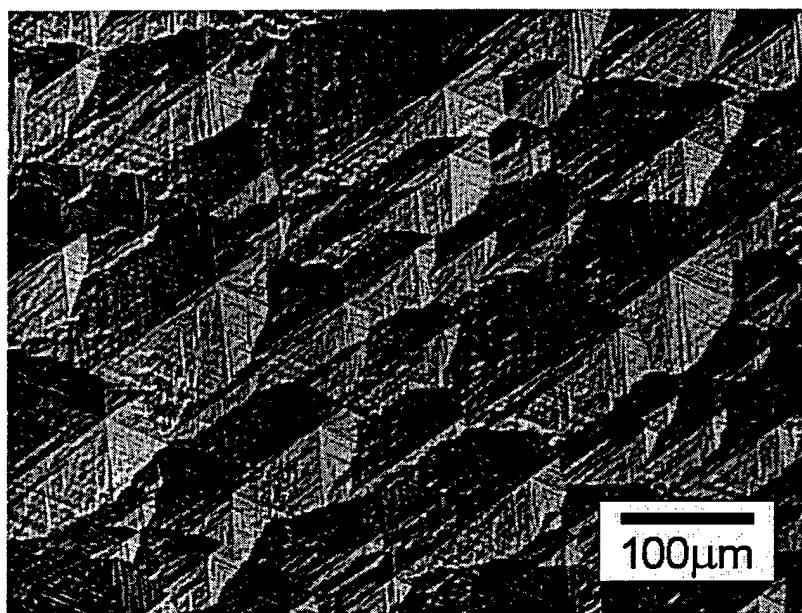
Figure 5.9a GaN Sample Grown Using Hydrogen Carrier Gas Showing Hexagonal Morphology
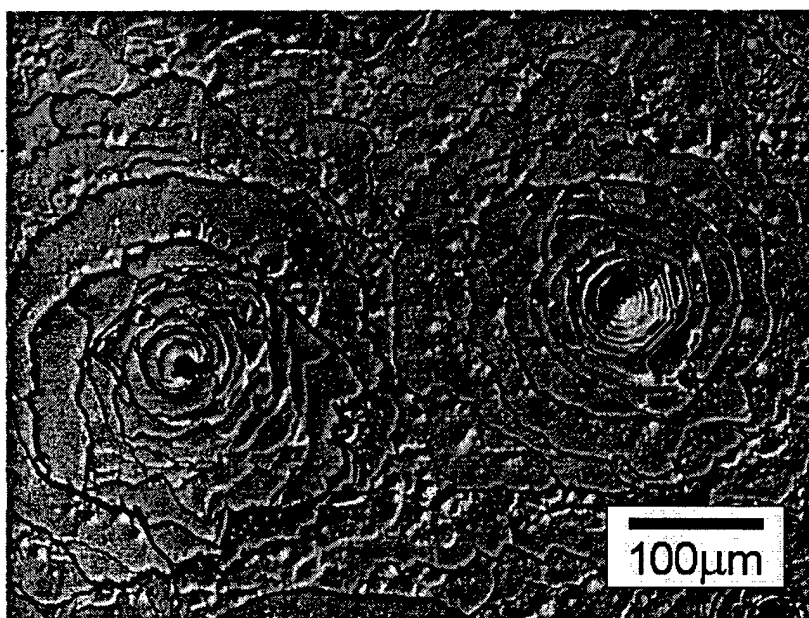
Figure 5.9b GaN Sample Grown Using Hydrogen Carrier Gas Showing "Volcano" Morphology
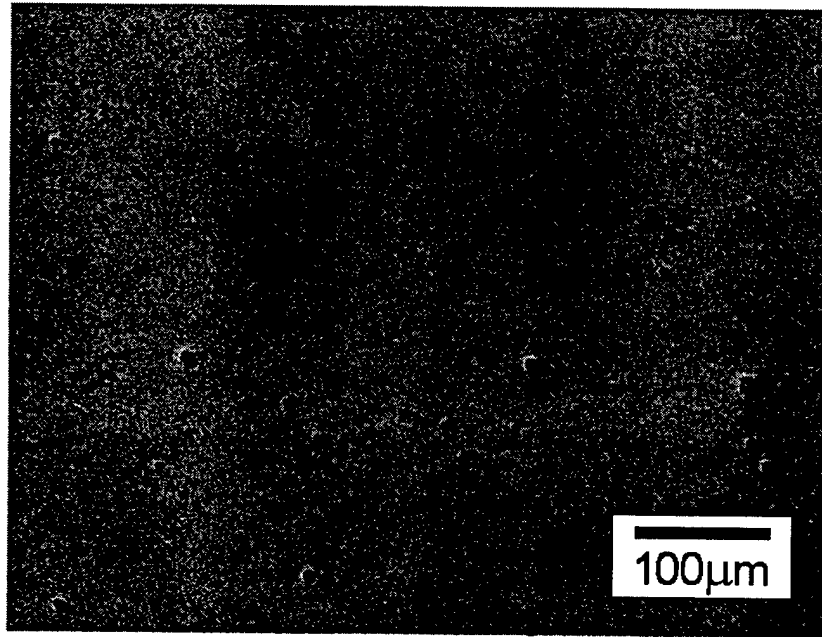
Figure 5.10a 150X Nomarski Image of AlN Sample Grown at 1000°C
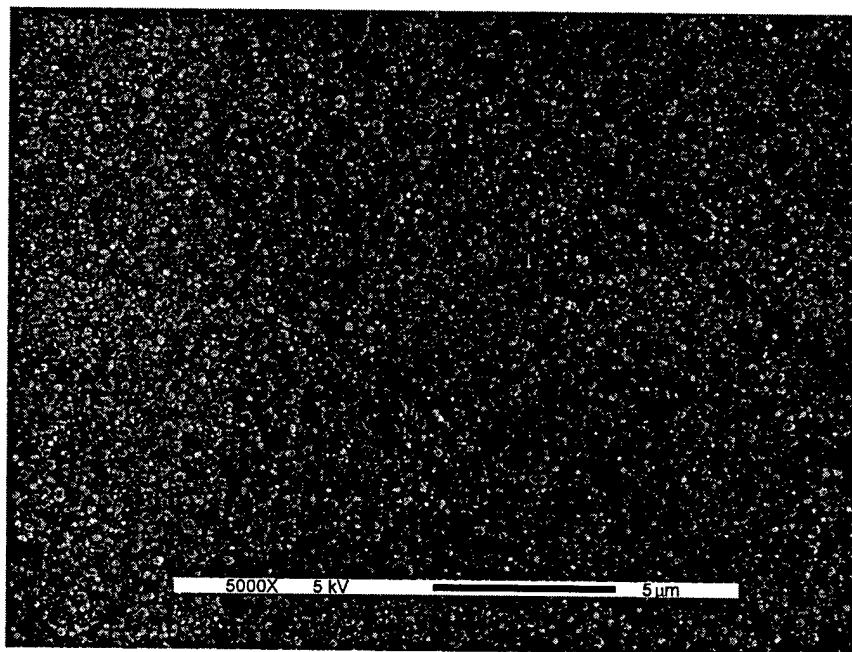
Figure 5.10b 5000X SEM Image of AlN Sample Grown at 1000°C
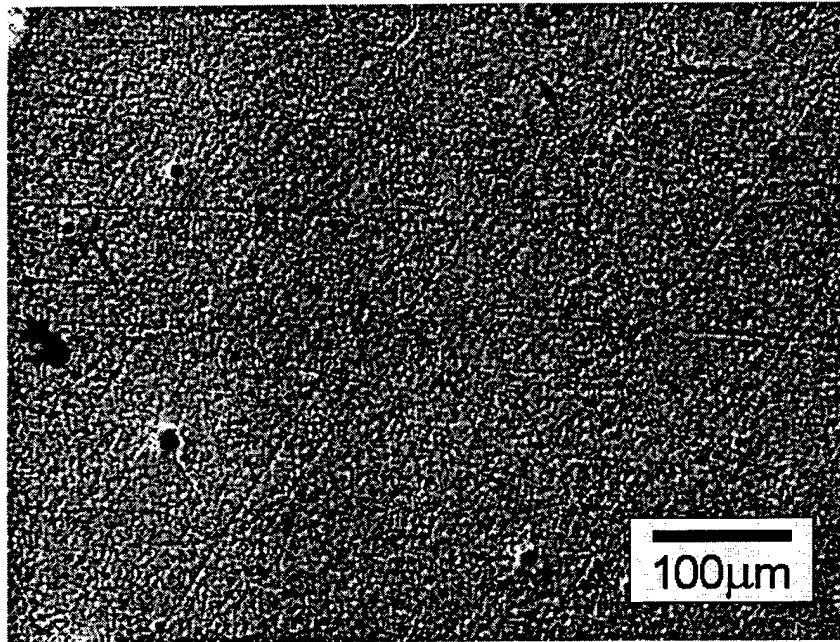
Figure 5.11a 150X Nomarski Image of AlN Sample Grown at 1160°C
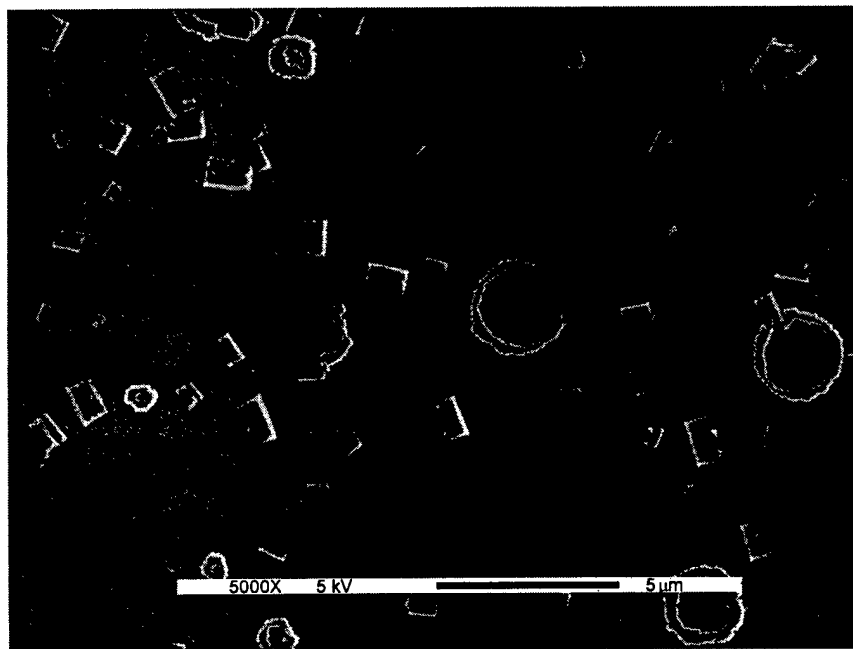
Figure 5.11b 5000X SEM Image of AlN Sample Grown at 1160°C
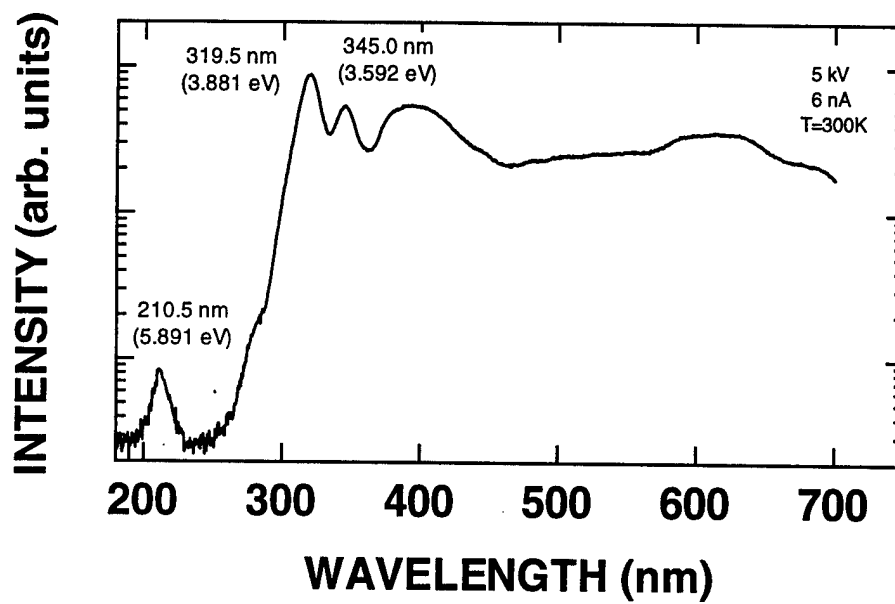
Figure 5.12a CL from AlN Grown at 1000°C
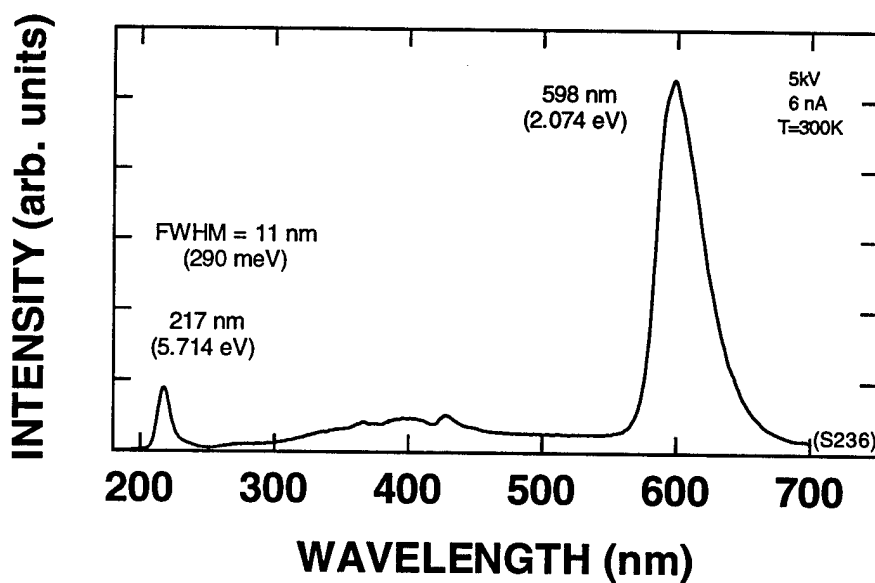
Figure 5.12b CL from AlN Grown at 1160°C

FWHM = 484 "

(S141)
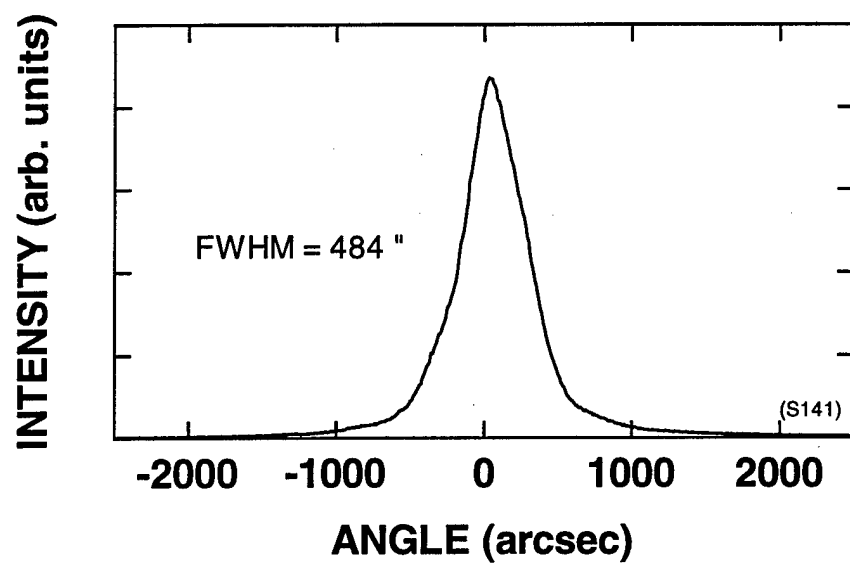
Figure 5.13a DXRC of AlN Grown at Low Temperature
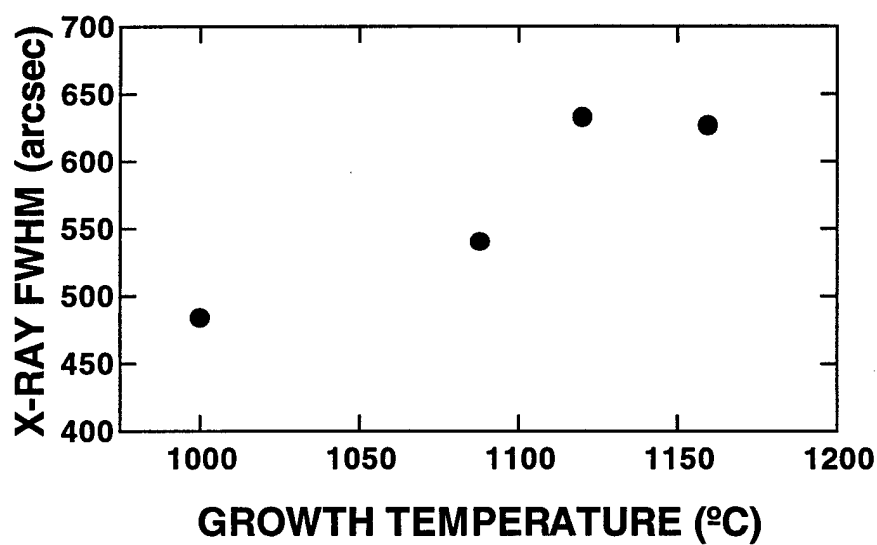
Figure 5.13b Dependence of AlN X-ray FWHM on Growth Temperature
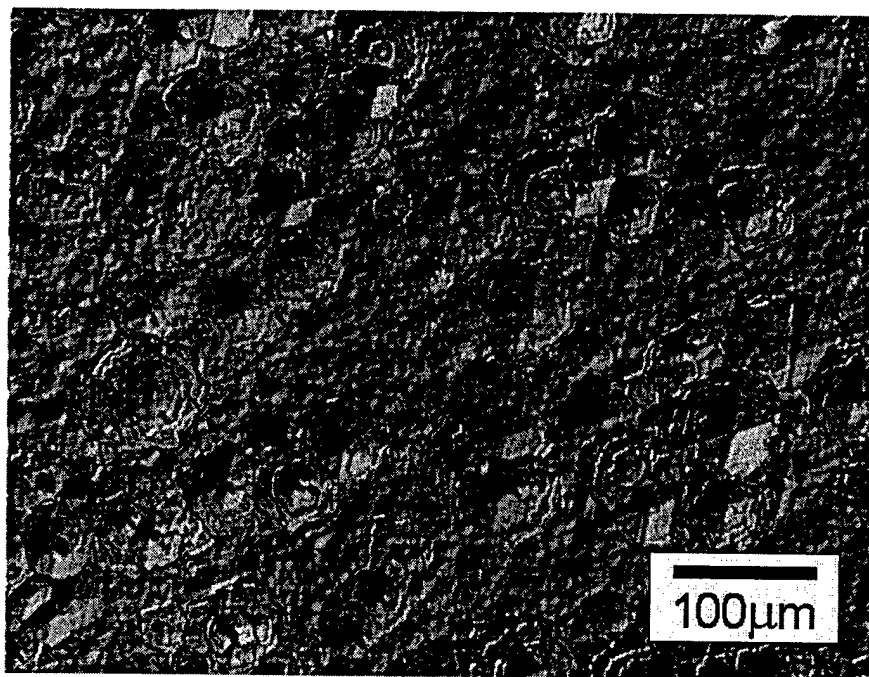
Figure 5.14 150X Nomarski Image of AlGaN Sample S165
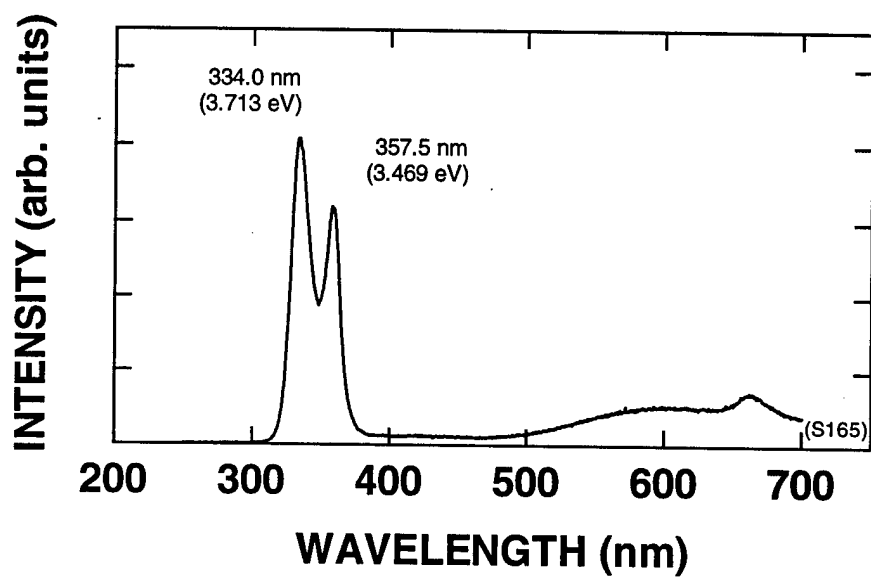
Figure 5.15 CL Spectrum of AlGaN Sample S165
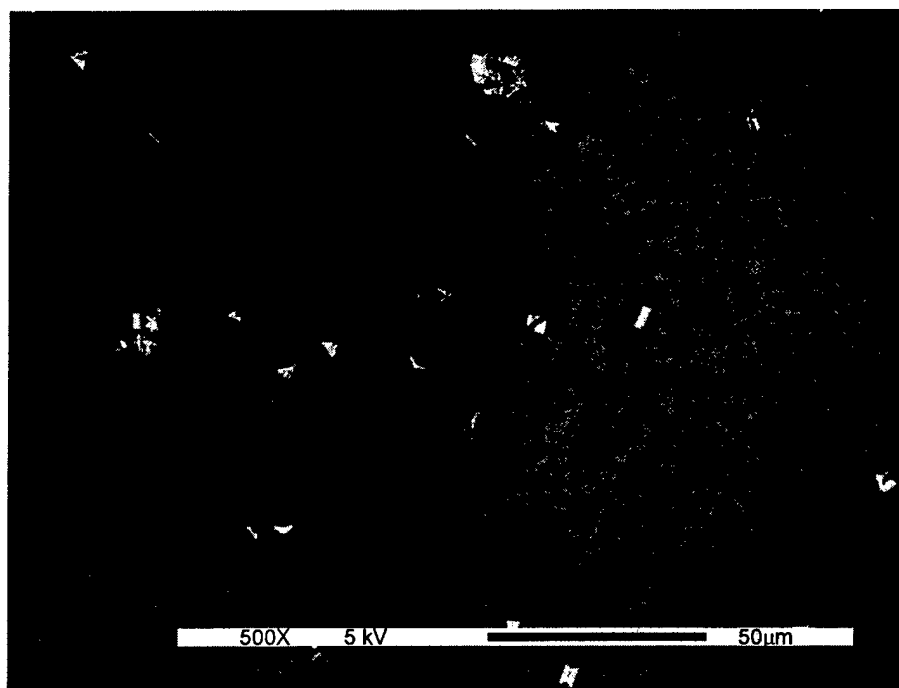
Figure 5.16a 334 nm CL Image of S165
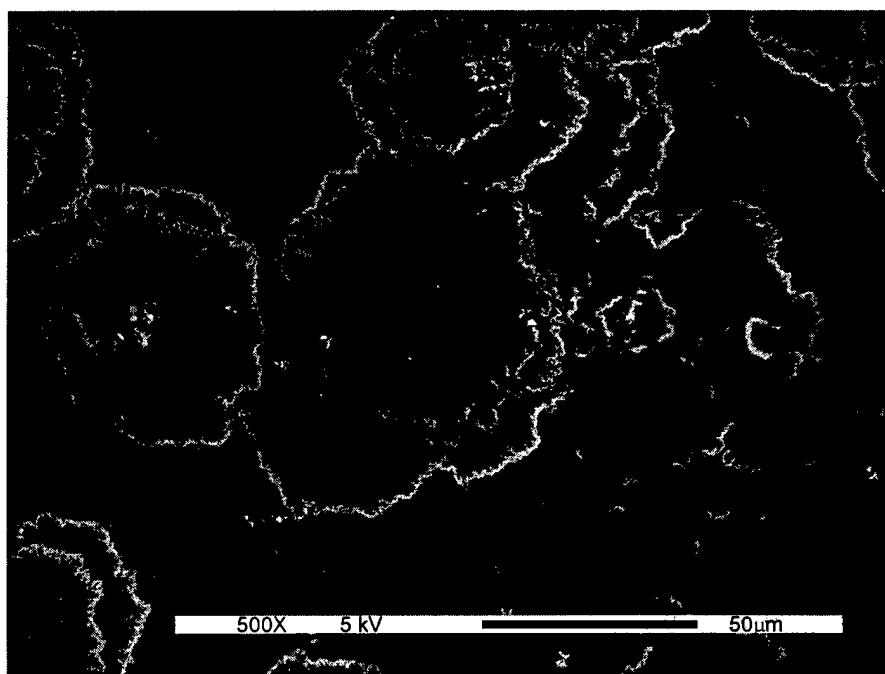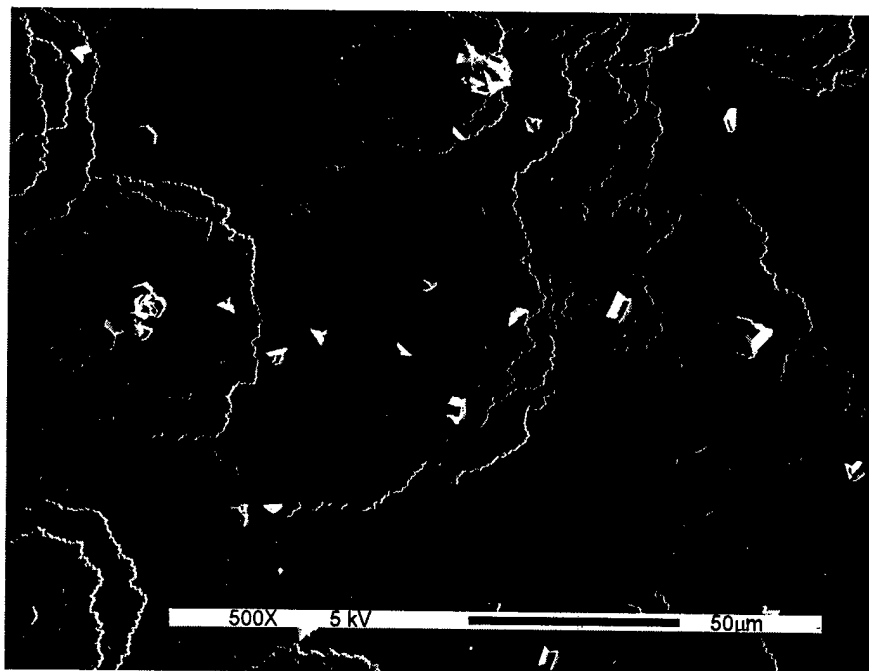

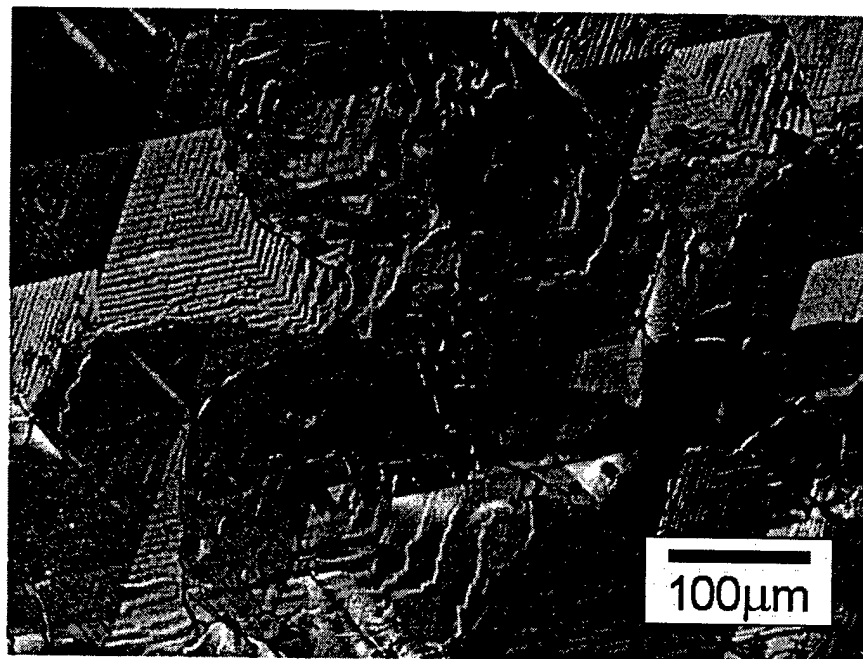Figure 5.16b 358 nm CL Image of S165

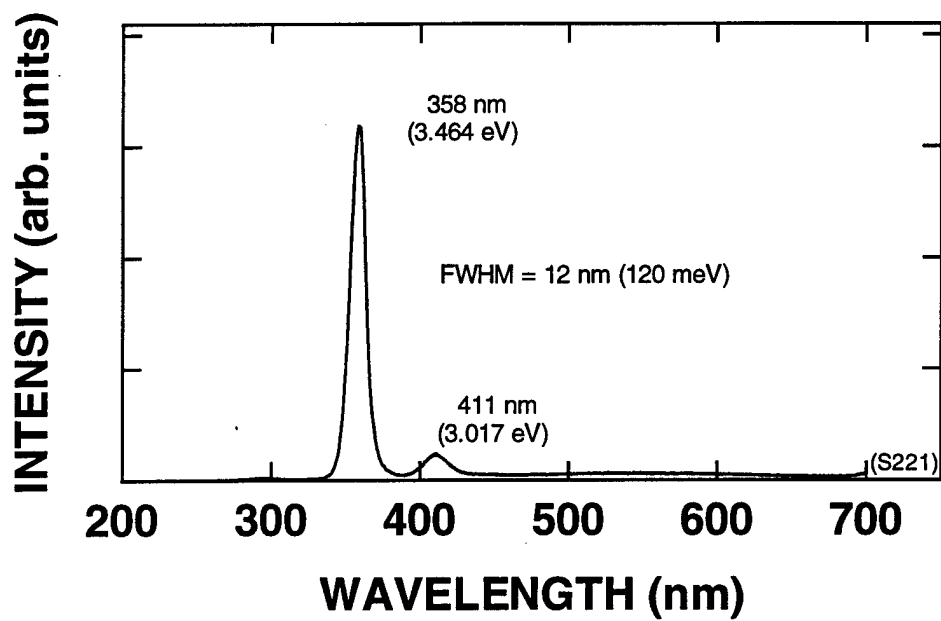Figure 5.16c SEM Image of CL Region

Figure 5.17 150X Nomarski Image of AlGaN Sample S221

Figure 5.18 CL Spectrum of AlGaN Sample S221